

Inverse Moment Matching Based Analysis of Cooperative HARQ-IR over Time-Correlated Nakagami Fading Channels

Zheng Shi, Haichuan Ding, Shaodan Ma, Kam-Weng Tam, and Su Pan

Abstract—This paper analyzes the performance of cooperative hybrid automatic repeat request with incremental redundancy (HARQ-IR) and proposes a new approach of outage probability approximation for performance analysis. A general time-correlated Nakagami fading channel covering fast fading and Rayleigh fading as special cases is considered here. An efficient inverse moment matching method is proposed to approximate the outage probability in closed-form. The effect of approximation degree is theoretically analyzed to ease its selection. Moreover, diversity order of cooperative HARQ-IR is analyzed. It is proved that diversity order is irrelevant to the time correlation coefficient ρ as long as $\rho < 1$ and full diversity from both spatial and time domains can be achieved by cooperative HARQ-IR under time-correlated fading channels. The accuracy of the analytical results is verified by computer simulations and the results reveal that cooperative HARQ-IR scheme can benefit from high fading order and low channel time correlation. Optimal rate selection to maximize the long term average throughput given a maximum allowable outage probability is finally discussed as one application of the analytical results.

Index Terms—HARQ-IR, time-correlated Nakagami-m fading, inverse moment matching, diversity order.

I. INTRODUCTION

IN wireless communications, wireless signals are generally corrupted by noise, interference and channel fading, etc. To boost the performance of wireless communications, a lot of techniques have been proposed in the past few decades. One promising technique proposed lately is cooperative relaying. It exploits spatial diversity to improve system capacity. Another promising technique is hybrid automatic repeat request (HARQ). It combines automatic repeat request (ARQ) and forward error correction (FEC) techniques to combat the detrimental effect of fading and noise [1]. Essentially, time diversity and coding gain are exploited for performance enhancement. Basically, there are three types of HARQ: Type-I HARQ, HARQ with chase combining (HARQ-CC) [2] and HARQ with incremental redundancy (HARQ-IR) [3]. Among them, HARQ-IR can provide superior performance due to the exploration of extra coding gaining through code combining. Clearly, by combining HARQ-IR with cooperative relaying,

not only spatial diversity but also time diversity and coding gain can be exploited to boost the communication performance further. Cooperative HARQ-IR thus has attracted considerable research interest recently [4]–[8].

To fully exploit the benefits of cooperative HARQ-IR and provide a theoretical guidance for system design, performance analysis of cooperative HARQ-IR is necessary and meaningful. Some analytical results have been reported in the literature. For instance, an opportunistic relaying HARQ-IR system is investigated and average throughput as well as outage probability are particularly analyzed in [4]. Since it considers a quasi-static Rayleigh fading channel wherein the channel responses corresponding to all HARQ rounds of a single packet are constant, the analysis is only applicable to a low mobility environment. For high mobility environment, communication channels are usually fast fading, i.e., all HARQ rounds experience independent channel realizations. Under such channels, an upper bound of outage probability is derived for a cooperative HARQ-IR system with a single relay using Jensen’s inequality in [5]. Optimal design to maximize the energy efficiency given an outage constraint is then discussed. Similarly, energy efficiency of a cooperative HARQ-IR system with distributed cooperative beamforming (DCB) is analyzed in [6]. With the analytical results, the optimal number of selected relays for DCB under a certain energy efficiency criterion is found. Regarding to a cooperative HARQ-IR enabled uplink cellular system, [7] derives the outage probability using Gaussian approximation, based on which a base station selection scheme is proposed. Considering the limitations of [5]–[7] where certain approximations are applied in the analysis, [8] derives the exact outage probability of cooperative HARQ-IR in terms of the generalized Fox’s H function. It enables further analysis of the average number of transmissions and the long term average throughput (LTAT) in closed-forms.

As aforementioned, most of prior works consider either quasi-static fading channels [4] or fast fading channels [5]–[8]. They are not applicable to time-correlated fading channels which usually occur in low-to-medium mobility environment. Under time-correlated fading channels, performance analysis of cooperative HARQ-IR becomes challenging due to the involvement of the product of multiple correlated random variables (RVs). It is also essentially different from the analysis of HARQ-CC over time-correlated fading channels in [9]–[11] where a sum of multiple correlated RVs is concerned. To our best knowledge, only few analytical results of HARQ-

Zheng Shi, Shaodan Ma and Kam-Weng Tam are with the Department of Electrical and Computer Engineering, University of Macau, Macao (e-mail: shizheng0124@gmail.com, shaodanma@umac.mo, kentam@umac.mo).

Haichuan Ding was with University of Macau, and is now with the Department of Electrical and Computer Engineering, University of Florida, U.S.A. (email: dhcbit@gmail.com).

Su Pan is with Nanjing University of Posts and Telecommunications, China (email: supan@njupt.edu.cn).

IR over time-correlated fading channels are available in [12] and [13]. Specifically, in [12], non-cooperative HARQ-IR operating over time-correlated Rayleigh fading channels is analyzed and outage probability is derived in closed-form based on polynomial fitting technique. On the other hand, outage probability of opportunistically relaying HARQ-IR operating over time-correlated Nakagami fading channels is derived based on a Lognormal approximation in [13]. Since the Lognormal approximation is developed based on central limit theorem (CLT) which is valid for independent fading channels, the analytical result in [13] is not accurate for channels with medium-to-high time correlation.

In this paper, we take a step further to analyze cooperative HARQ-IR operating over general time-correlated Nakagami fading channels. Notice that Nakagami fading is more general than Rayleigh fading and covers Rayleigh fading as a special case with fading order of 1. Due to the involvement of cooperative relaying and Nakagami distribution, the analytical approach in [12] can not be directly applied here. Since the outage probability can be written as cumulative distribution function (CDF) of a product of multiple correlated RVs, it is essential to determine the CDF of the product of multiple correlated RVs. After proving its inverse moments are bounded, we find that the CDF can be uniquely determined by matching the inverse moments. An efficient inverse moment matching approximation is then proposed to derive the outage probability in closed-form and the effect of approximation degree is theoretically analyzed. It is found that the outage probability can be eventually derived as a weighted sum of the CDFs of Lognormal RVs and the Lognormal approximation in [13] in fact is a special case of our analysis with approximation degree of zero. Diversity order of cooperative HARQ-IR is also investigated. It is proved that full diversity can be achieved by cooperative HARQ-IR under time-correlated fading channels, except fully correlated fading channels (i.e., quasi-static fading channels). Our analytical results are then verified through Monte Carlo simulations. It is shown that our analytical approach performs better than that in [13]. It is also revealed that low time correlation and high fading order are beneficial to the system performance. Our analytical results can facilitate the system design to achieve various objectives, e.g., the maximization of long term average throughput, the minimization of average number of transmissions and the minimization of outage probability, etc.. Optimal rate selection to maximize the long term average throughput given different outage constraints is finally discussed as an example.

The rest of this paper is organized as follows. In Section II, cooperative HARQ-IR protocol and general time-correlated Nakagami fading channels are introduced. Inverse moment matching method is introduced and the outage probability is derived in Section III, while diversity order of cooperative HARQ-IR is investigated in Section IV. In Section V, the accuracy of our analytical results is verified and optimal rate selection is discussed as an example. Finally, conclusions are drawn in Section VI.

II. SYSTEM MODEL

A cooperative system including one source node, one relay node and one destination node, is considered as shown in Fig. 1. To improve the transmission reliability, HARQ-IR protocol is adopted in each node. Unlike prior analyses, a general time-correlated fading channel which covers the fast fading channel as a special case is considered. In the following, the cooperative HARQ-IR protocol and time-correlated fading channel model are introduced in detail.

A. Cooperative HARQ-IR Protocol

Following the HARQ-IR protocol, every b -bits information message at the source is encoded into a codeword with $M \times L$ symbols [2], where M is the maximal allowable number of HARQ transmissions. The codeword is then chopped into M sub-codewords, i.e., $\{C_1, \dots, C_l, \dots, C_M\}$, each with length L for transmission in one HARQ round.

The cooperative HARQ-IR transmission consists of two phases, i.e., broadcasting and relaying phases, as shown in Fig. 1. During the broadcasting phase, the source sequentially transmits sub-codewords to both the destination and the relay until the maximum number of transmissions is reached or an acknowledgement (ACK) of successful decoding is received from the destination/relay. If the destination successfully decodes the message before the relay, an ACK message will be fed back from the destination to the source and it will be overheard by the relay. The message transmission then completes without moving to the relaying phase. On the contrary, an ACK message will be fed back from the relay and the source will move to the relaying phase. During the relaying phase, the relay encodes the successfully decoded message again and transmits the subsequent sub-codewords to the destination until the maximum number of transmissions is reached or an ACK from the destination is received. The transmitted sub-codewords are different from that transmitted by the source in the broadcasting phase. The destination will use all of the received sub-codewords in both the broadcasting and relaying phases for decoding. In the meanwhile, the source oversees the transmission and listens to the feedback. Once an ACK message is received by the source or the maximum number of transmissions is reached, the transmission for the next b bits information message will be initiated and a new cooperative HARQ-IR transmission will be started. Here an error-free feedback channel is assumed available as [14], [15], that is, all feedback messages can be correctly decoded.

B. Channel Model

In the broadcasting phase, the received signals at the destination and at the relay in the l -th HARQ round can be written respectively as

$$\mathbf{y}_{SD,l} = h_{SD,l} \sqrt{P_{S,l}} \mathbf{x}_l + \mathbf{n}_{SD,l}, \quad (1)$$

$$\mathbf{y}_{SR,l} = h_{SR,l} \sqrt{P_{S,l}} \mathbf{x}_l + \mathbf{n}_{SR,l}, \quad (2)$$

where \mathbf{x}_l corresponds to the l -th sub-codeword C_l and denotes the transmitted signal with unit power in the l -th HARQ round; $P_{S,l}$ represents the transmission power in the l -th

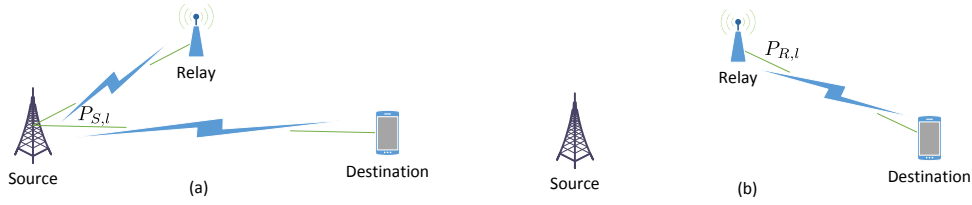


Fig. 1. A cooperative HARQ-IR system. (a) Broadcasting phase (b) Relaying phase.

HARQ round; $\mathbf{n}_{SD,l}$ and $\mathbf{n}_{SR,l}$ represent zero mean additive white Gaussian noises (AWGNs) with variances $\mathfrak{N}_{SD,l}$ and $\mathfrak{N}_{SR,l}$, respectively; and $h_{SD,l}$ and $h_{SR,l}$ signify the channel coefficients associated with the source-to-destination and the source-to-relay links in the l -th HARQ round, respectively.

In the relaying phase, only the relay is involved in the transmission of the subsequent sub-codewords. Accordingly, the received signal at the destination in the l -th HARQ round is expressed as

$$\mathbf{y}_{RD,l} = h_{RD,l} \sqrt{P_{R,l}} \mathbf{x}_l + \mathbf{n}_{RD,l}, \quad (3)$$

where $P_{R,l}$ represents the transmission power at the relay in the l -th HARQ round; $\mathbf{n}_{RD,l}$ denotes zero mean AWGN with variance $\mathfrak{N}_{RD,l}$; and $h_{RD,l}$ represents the channel coefficient corresponding to the relay-to-destination link.

For notational convenience, we use $h_{ab,l}$ to unify the channel coefficients $h_{SD,l}$, $h_{SR,l}$ and $h_{RD,l}$, where $(a, b) \in \{(S, D), (S, R), (R, D)\}$. Different from prior analyses [6], [8], [15], channel time correlation is considered here. Specifically, general time-correlated Nakagami- m fading channels are considered, i.e., the channel coefficients in multiple HARQ rounds $h_{ab,1}, \dots, h_{ab,M}$ are correlated. The amplitudes of the channel coefficients are modeled as multivariate Nakagami- m distributed random variables (RVs) with generalized correlation. The joint probability density function (PDF) corresponding to $|\mathbf{h}_{ab}| = (|h_{ab,1}|, |h_{ab,2}|, \dots, |h_{ab,M}|)$ is given by [16]

$$\begin{aligned} f_{|\mathbf{h}_{ab}|}(x_1, \dots, x_M) &= \int_{t=0}^{\infty} \frac{t^{m-1}}{\Gamma(m)} e^{-t} \\ &\times \prod_{l=1}^M \frac{2x_l^{2m-1}}{\Gamma(m) \left(\frac{\Omega_{ab,l}(1-\lambda_{ab,l}^2)}{m}\right)^m} e^{-\frac{mx_l^2}{\Omega_{ab,l}(1-\lambda_{ab,l}^2)}} e^{-\frac{\lambda_{ab,l}^2 t}{1-\lambda_{ab,l}^2}} \\ &\times {}_0F_1\left(; m; \frac{mx_l^2 \lambda_{ab,l}^2 t}{\Omega_{ab,l}(1-\lambda_{ab,l}^2)^2}\right) dt, \quad |\lambda_{ab,l}| < 1, \quad (4) \end{aligned}$$

where m denotes the Nakagami fading order which determines the severity of the fading, $\Omega_{ab,l}$ is the mean channel power gain, i.e., $\Omega_{ab,l} = \mathbb{E}(|h_{ab,l}|^2)$, $\lambda_{ab,l}$ denotes generalized correlation coefficient, $\Gamma(\cdot)$ represents Gamma function and ${}_0F_1(\cdot)$ denotes the confluent hypergeometric limit function [17, Eq. 9.14.1]. Notice that the time-correlated Rayleigh fading channel in [12] is a special case of this channel model with $m = 1$. Moreover, the correlation coefficient $\lambda_{ab,l}$ specifies the cross correlation coefficient $\rho_{ab}^{l,k}$ between

the squared channel amplitudes $|h_{ab,l}|^2$ and $|h_{ab,k}|^2$ as [16]

$$\begin{aligned} \rho_{ab}^{l,k} &= \frac{\mathbb{E}(|h_{ab,l}|^2 |h_{ab,k}|^2) - \mathbb{E}(|h_{ab,l}|^2) \mathbb{E}(|h_{ab,k}|^2)}{\sqrt{\text{Var}(|h_{ab,l}|^2) \text{Var}(|h_{ab,k}|^2)}} \\ &= \lambda_{ab,l}^2 \lambda_{ab,k}^2, \quad 1 \leq l \neq k \leq M, \quad (5) \end{aligned}$$

where $\text{Var}(\cdot)$ denotes the operation of variance. It is noteworthy that $|\lambda_{ab,l}| < 1$ in (4), thus $\rho_{ab}^{l,k} < 1$. This channel model covers fast fading channels where the channel coefficients are independent with cross correlation $\rho_{ab}^{l,k} = 0$ as a special case. It is not applicable to quasi-static fading channels where $h_{ab,1} = h_{ab,2} = \dots = h_{ab,M}$ and $\rho_{ab}^{l,k} = 1$. The analysis for quasi-static fading channels has been discussed in [4]. Clearly from (4), the channel amplitude $|h_{ab,l}|$ follows Nakagami- m distribution (i.e., $|h_{ab,l}| \sim \text{Nakagami}(m, \Omega_{ab,l})$) with a PDF of

$$f_{|h_{ab,l}|}(x) = \frac{2m^m x^{2m-1}}{(\Omega_{ab,l})^m \Gamma(m)} \exp\left(-\frac{m}{\Omega_{ab,l}} x^2\right), \quad x \in [0, +\infty). \quad (6)$$

Herein, it should be noted that the channel coefficients associated with different links are independent, that is, \mathbf{h}_{SD} , \mathbf{h}_{SR} and \mathbf{h}_{RD} are mutually independent.

Accordingly, the received signal-to-noise ratio (SNR) in the l -th HARQ round associated with the link between a and b is written as

$$\gamma_{ab,l} = \frac{P_{a,l} |h_{ab,l}|^2}{\mathfrak{N}_{ab,l}}, \quad (7)$$

and follows Gamma distribution, i.e., $\gamma_{ab,l} \sim \mathcal{G}(m, \Omega'_{ab,l}/m)$ where $\Omega'_{ab,l} = \Omega_{ab,l} P_{a,l} / \mathfrak{N}_{ab,l}$. By using (4) and making changes of variables, it is readily proved that the joint distribution of $\gamma_{ab} = (\gamma_{ab,1}, \dots, \gamma_{ab,M})$ complies with multivariate Gamma distribution with generalized correlation. More specifically, the joint PDF of γ_{ab} can be derived as

$$\begin{aligned} f_{\gamma_{ab}}(\gamma_1, \dots, \gamma_M) &= \int_{t=0}^{\infty} \frac{t^{m-1}}{\Gamma(m)} e^{-t} \\ &\times \prod_{l=1}^M \frac{\gamma_l^{m-1}}{\Gamma(m) \left(\frac{\Omega'_{ab,l}(1-\lambda_{ab,l}^2)}{m}\right)^m} e^{-\frac{m\gamma_l}{\Omega'_{ab,l}(1-\lambda_{ab,l}^2)}} e^{-\frac{\lambda_{ab,l}^2 t}{1-\lambda_{ab,l}^2}} \\ &\times {}_0F_1\left(; m; \frac{m\gamma_l \lambda_{ab,l}^2 t}{\Omega'_{ab,l}(1-\lambda_{ab,l}^2)^2}\right) dt, \quad |\lambda_{ab,l}| < 1. \quad (8) \end{aligned}$$

Due to the presence of time correlation in the channel coefficients, the analysis becomes much more challenging than the prior works in the literature.

III. OUTAGE ANALYSIS

The most fundamental performance metric for various HARQ schemes is outage probability. It can well approximate the error probability when Gaussian codes and typical set decoding are applied [18]. In HARQ-IR scheme, message decoding is performed based on the signals received in all the previous HARQ rounds. Outage would happen when the accumulated mutual information per symbol is less than the initial transmission rate \mathcal{R} [19]. Since the cooperative HARQ-IR scheme involves both broadcasting and relaying phases, the destination can acquire information from both the source and the relay. The outage probability at the destination after K HARQ rounds can thus be expressed based on the Total Probability theorem as [8], [20]

$$P_{out}(K) = \sum_{r=1}^K P_{out}(K|BC=r) \Pr(BC=r), \quad (9)$$

where $P_{out}(K|BC=r)$ denotes the conditional outage probability given there are r broadcasting HARQ rounds among the K HARQ rounds, while $\Pr(BC=r)$ is the probability that r out of K HARQ rounds are in the broadcasting phase.

Similarly to [18], we assume Gaussian codes are applied and channel state information is perfectly known at the receivers. As mentioned in the cooperative protocol, the destination acquires information only from the source in the broadcasting phase, while it gets information only from the relay in the relaying phase. The conditional outage probability $P_{out}(K|BC=r)$ thus can be written as [8], [18], [20]

$$P_{out}(K|BC=r) = \Pr(I_{K,r} \leq \mathcal{R}), \quad (10)$$

where $I_{K,r}$ is given as [21], [22]

$$\begin{aligned} I_{K,r} &= \frac{1}{L} I(\mathbf{x}_1, \dots, \mathbf{x}_K; \\ &\quad \mathbf{y}_{SD,1}, \dots, \mathbf{y}_{SD,r}, \mathbf{y}_{RD,r+1}, \dots, \mathbf{y}_{RD,K} | \mathbf{h}_{K,r}) \\ &\stackrel{(a)}{=} \frac{1}{L} \left\{ \sum_{l=1}^r I(\mathbf{x}_l; \mathbf{y}_{SD,l} | h_{SD,l}) + \sum_{l=r+1}^K I(\mathbf{x}_l; \mathbf{y}_{RD,l} | h_{RD,l}) \right\} \\ &= \sum_{l=1}^r \log_2(1 + \gamma_{SD,l}) + \sum_{l=r+1}^K \log_2(1 + \gamma_{RD,l}), \end{aligned} \quad (11)$$

where L is the number of symbols in each sub-codeword, $\mathbf{h}_{K,r} = \{h_{SD,1}, \dots, h_{SD,r}, h_{RD,r+1}, \dots, h_{RD,K}\}$, $I(\mathbf{x}; \mathbf{y} | \mathbf{z})$ denotes the conditional mutual information of random variables \mathbf{x} and \mathbf{y} given \mathbf{z} , and (a) holds since the inputs $\mathbf{x}_1, \dots, \mathbf{x}_K$ are independent and the channels are memoryless. It follows the conditional outage probability as

$$P_{out}(K|BC=r) = \begin{cases} \Pr \left(\sum_{l=1}^r \log_2(1 + \gamma_{SD,l}) + \sum_{l=r+1}^K \log_2(1 + \gamma_{RD,l}) < \mathcal{R} \right) & r < K \\ \Pr \left(\sum_{l=1}^K \log_2(1 + \gamma_{SD,l}) < \mathcal{R} \right) & r = K. \end{cases} \quad (12)$$

After simple manipulation, it can be rewritten as

$$P_{out}(K|BC=r) = \begin{cases} \Pr \left(Y_{K,r}^D \triangleq \prod_{l=1}^r (1 + \gamma_{SD,l}) \times \prod_{l=r+1}^K (1 + \gamma_{RD,l}) < 2^{\mathcal{R}} \right) & r < K \\ \Pr \left(Y_K^D \triangleq \prod_{l=1}^K (1 + \gamma_{SD,l}) < 2^{\mathcal{R}} \right) & r = K. \end{cases} \quad (13)$$

On the other hand, since the relaying phase starts only when the relay can successfully decode the message, i.e., the accumulated mutual information per symbol at the relay is not less than the transmission rate \mathcal{R} , the probability $\Pr(BC=r)$ can similarly be written as

$$\Pr(BC=r) = \begin{cases} \Pr \left(\sum_{l=1}^{r-1} \log_2(1 + \gamma_{SR,l}) < \mathcal{R}, \sum_{l=r}^K \log_2(1 + \gamma_{SR,l}) \geq \mathcal{R} \right) & K > r \geq 1 \\ \Pr \left(\sum_{l=1}^{K-1} \log_2(1 + \gamma_{SR,l}) < \mathcal{R} \right) & K = r \geq 1. \end{cases} \quad (14)$$

By defining $Y_r^R \triangleq \prod_{l=1}^r (1 + \gamma_{SR,l})$ and $Y_0^R \triangleq 0$, it can be rewritten as

$$\Pr(BC=r) = \begin{cases} \Pr(Y_{r-1}^R < 2^{\mathcal{R}}) - \Pr(Y_r^R < 2^{\mathcal{R}}) & K > r \geq 1 \\ \Pr(Y_{K-1}^R < 2^{\mathcal{R}}) & K = r \geq 1. \end{cases} \quad (15)$$

Clearly from (9), (13) and (15), the CDFs of the products of multiple shifted SNRs, i.e., $Y_{K,r}^D$, Y_K^D , and Y_r^R , are essential for the outage analysis. In the literature, there are two kinds of approaches to derive the CDF of the product of multiple RVs: Mellin transform [8] and moment matching method [23], [24]. Mellin transform is effective for the case with independent RVs and however is inapplicable to our analysis since the multiple SNRs are correlated due to the channel time correlation [25]. On the other hand, although the moments of the products of multiple shifted SNRs (i.e., $Y_{K,r}^D$, Y_K^D , and Y_r^R) exist, their moment generation functions (MGFs) do not exist when the number of transmissions K or r is larger than one as proved in Appendix A. According to [26, pp. 176-177], the uniqueness of the CDFs thus can not be guaranteed by matching the moments of $Y_{K,r}^D$, Y_K^D , and Y_r^R when $K, r > 1$, which would result in notable degradation on the accuracy of outage analysis based on moment matching method.

Fortunately, after analyzing the products of multiple shifted SNRs, we found that their inverse moments do have special properties which can facilitate the derivation and guarantee the uniqueness of their CDFs. Based on these findings, we will propose an effective outage analysis approach based on inverse moment matching method. In the following, the details of inverse moment matching method will be first introduced by taking the analysis of the CDF of Y_K^D as an example. The derivations of the CDFs of Y_r^R and $Y_{K,r}^D$ will be briefly introduced later.

A. Inverse Moment Matching Method

Denote the PDF of the product of multiple shifted SNRs corresponding to the source-to-destination link Y_K^D as $f_{Y_K^D}(y)$. The inverse moment of Y_K^D is defined as $\alpha_n = \mathbb{E}\{(Y_K^D)^{-n}\} = \int_0^\infty y^{-n} f_{Y_K^D}(y) dy$. As shown in Appendix B, it can be explicitly derived as

$$\alpha_n \approx \sum_{p_1, \dots, p_K \in [1, N_Q]} \frac{\prod_{l=1}^K w_{p_l} \left(1 + \frac{\Omega'_{SD,l}(1-\lambda_{SD,l}^2)\zeta_{p_l}}{m}\right)^{-n}}{\Gamma(m) \left(1 + \sum_{l=1}^K \frac{\lambda_{SD,l}^2}{1-\lambda_{SD,l}^2}\right)^m} \times \Psi_2^{(K)}(m; m, \dots, m; \varpi_1 \zeta_{p_1}, \dots, \varpi_K \zeta_{p_K}), \quad (16)$$

where $\varpi_l = \left(1 + \sum_{k=1}^K \frac{\lambda_{SD,k}^2}{1-\lambda_{SD,k}^2}\right)^{-1} \frac{\lambda_{SD,l}^2}{1-\lambda_{SD,l}^2}$, N_Q is the quadrature order, the weights w_{p_l} and abscissas ζ_{p_l} for N_Q up to 32 are tabulated in [27], and $\Psi_2^{(K)}(; ;)$ denotes the confluent form of Lauricella hypergeometric function [28, Definition A.20]. Moreover, the inverse moment α_n has the following property.

Property 1. *The inverse moment α_n is bounded in $(0, 1]$ and decreases with n . The series $\sum_{n=0}^\infty \alpha_n s^n / n!$ absolutely converges for some $s > 0$.*

Proof. According to the definition of Y_K^D , it is clear that $Y_K^D \geq 1$ and the inverse moment α_n decreases to zero with n , i.e.,

$$0 < \alpha_n < \alpha_{n-1} < \dots < \alpha_0 = 1. \quad (17)$$

It follows that

$$\sum_{n=0}^\infty |\alpha_n s^n / n!| \leq \sum_{n=0}^\infty |s|^n / n! = e^{|s|}, \quad (18)$$

which means that the series $\sum_{n=0}^\infty \alpha_n s^n / n!$ absolutely converges for some $s > 0$ according to Lebesgue's monotone convergence theorem. \square

Meanwhile, we have the following lemma about inverse moments from [29].

Lemma 1. [29, Result 4.14] *For any RV Y with CDF of $F_Y(y)$, if its inverse moments $\alpha_0 = 1, \alpha_1, \dots$, are finite and the series $\sum_{n=0}^\infty \alpha_n s^n / n!$ is absolutely convergent for some $s > 0$, its CDF $F_Y(y)$ is the only CDF having $\alpha_0, \alpha_1, \dots$, as its inverse moments.*

Based on Property 1 and Lemma 1, it can be concluded that the CDF of the product of multiple shifted SNRs corresponding to the source-destination link Y_K^D can be uniquely determined by matching its inverse moments α_n . The PDF $f_{Y_K^D}(y)$ can thus be uniquely determined as shown in the following theorem.

Theorem 1. *By matching the inverse moments α_n , the PDF $f_{Y_K^D}(y)$ can be uniquely expressed as*

$$f_{Y_K^D}(y) = f_b(y) \sum_{l=0}^\infty \xi_l y^{-l}, \quad (19)$$

where $f_b(y)$ is a nontrivial function of y and denotes a base density function with inverse moments $\nu_l = \int_{-\infty}^\infty y^{-l} f_b(y) dy$

existing for $l = 0, 1, \dots$, and the coefficients ξ_l match the inverse moments α_n such that

$$\alpha_n = \int_{-\infty}^\infty y^{-n} f_{Y_K^D}(y) dy = \sum_{l=0}^\infty \xi_l \nu_{n+l}, \quad n = 0, 1, \dots. \quad (20)$$

Proof. Please see Appendix C. \square

With the unique expression of the PDF $f_{Y_K^D}(y)$ in (19), the PDF can be approximated by truncating the series in (19) as

$$f_{Y_K^D}(y) \approx \tilde{f}_N(y) = f_b(y) \sum_{l=0}^N \xi_{N,l} y^{-l} = f_b(y) \boldsymbol{\xi}_N^T \mathbf{y}_N, \quad (21)$$

where N denotes the approximation degree, $\mathbf{y}_N = [1 \ y^{-1} \ \dots \ y^{-N}]^T$, and $\boldsymbol{\xi}_N = [\xi_{N,0} \ \dots \ \xi_{N,N}]^T$ is determined by matching the first $N+1$ inverse moments, i.e., $\alpha_0, \dots, \alpha_N$. Specifically, by matching the first $N+1$ inverse moments as (20), the coefficient vector $\boldsymbol{\xi}_N$ should satisfy

$$\mathbf{A}_N \boldsymbol{\xi}_N = \boldsymbol{\alpha}_N, \quad (22)$$

where

$$\mathbf{A}_N = \begin{bmatrix} \nu_0 & \nu_1 & \dots & \nu_N \\ \nu_1 & \nu_2 & \dots & \nu_{N+1} \\ \vdots & \vdots & \ddots & \vdots \\ \nu_N & \nu_{N+1} & \dots & \nu_{2N} \end{bmatrix}, \quad (23)$$

and $\boldsymbol{\alpha}_N = [1 \ \alpha_1 \ \alpha_2 \ \dots \ \alpha_N]^T$. For an arbitrary vector $\mathbf{d} = [d_0, \dots, d_N]^T$, we have $\mathbf{d}^T \mathbf{A}_N \mathbf{d} = \int_0^\infty f_b(y) \left(\sum_{l=0}^N d_l y^{-l}\right) dy \geq 0$ where the equality holds if and only if $\mathbf{d} = \mathbf{0}$. Therefore, the matrix \mathbf{A}_N is positive definite and invertible. From (22), it follows that

$$\boldsymbol{\xi}_N = \mathbf{A}_N^{-1} \boldsymbol{\alpha}_N. \quad (24)$$

Clearly from (24), matrix inversion is involved in the calculation of the coefficient vector in the approximated PDF. It has high complexity and also causes difficulty in the selection of approximation degree. To avoid that, the approximated PDF is reformulated as shown in the following theorem.

Theorem 2. *The approximated PDF can be reformulated as*

$$\tilde{f}_N(y) = f_b(y) \sum_{l=0}^N \eta_l \mathbf{c}_l^T \mathbf{y}_l, \quad (25)$$

where

$$\eta_l = \mathbf{c}_l^T \boldsymbol{\alpha}_l, \quad (26)$$

and

$$\mathbf{c}_l = \left[\frac{-\mathbf{v}_{l-1}^T \mathbf{A}_{l-1}^{-1}}{\sqrt{\nu_{2l} - \mathbf{v}_{l-1}^T \mathbf{A}_{l-1}^{-1} \mathbf{v}_{l-1}}} \quad \frac{1}{\sqrt{\nu_{2l} - \mathbf{v}_{l-1}^T \mathbf{A}_{l-1}^{-1} \mathbf{v}_{l-1}}} \right]^T. \quad (27)$$

In (27), $\mathbf{v}_l = [\nu_{l+1} \ \cdots \ \nu_{2l+1}]^T$, $\mathbf{c}_0 = [1]$, $\mathbf{A}_0 = [1]$, and \mathbf{A}_l^{-1} is given recursively as

$$\mathbf{A}_l^{-1} = \begin{bmatrix} \mathbf{A}_{l-1}^{-1} + \frac{\mathbf{A}_{l-1}^{-1} \mathbf{v}_{l-1} \mathbf{v}_{l-1}^T \mathbf{A}_{l-1}^{-1}}{\nu_{2l} - \mathbf{v}_{l-1}^T \mathbf{A}_{l-1}^{-1} \mathbf{v}_{l-1}} & \\ & -\frac{\mathbf{v}_{l-1}^T \mathbf{A}_{l-1}^{-1}}{\nu_{2l} - \mathbf{v}_{l-1}^T \mathbf{A}_{l-1}^{-1} \mathbf{v}_{l-1}} \\ & & \mathbf{A}_{l-1}^{-1} \mathbf{v}_{l-1} \\ & & & \frac{1}{\nu_{2l} - \mathbf{v}_{l-1}^T \mathbf{A}_{l-1}^{-1} \mathbf{v}_{l-1}} \end{bmatrix}. \quad (28)$$

Proof. Please see Appendix D. \square

Remark 1. As shown in Appendix E, the set $\{\mathbf{c}_l^T \mathbf{y}_l, l \in \mathbb{N}\}$ in (25) satisfies the orthogonality as

$$\langle \mathbf{c}_l^T \mathbf{y}_l, \mathbf{c}_k^T \mathbf{y}_k \rangle = \begin{cases} 0, & l \neq k; \\ 1, & l = k, \end{cases} \quad (29)$$

where $\langle g(y), h(y) \rangle$ defines an inner product on 2-norm Lebesgue spaces $L^2(\mathbb{R}, \mathcal{F}, u)^1$ with respect to a measure $dF_b(y) = f_b(y)dy$, such that

$$\langle g(y), h(y) \rangle = \int_0^\infty g(y) h(y) dF_b(y). \quad (30)$$

In other words, the set $\{\mathbf{c}_l^T \mathbf{y}_l, l \in \mathbb{N}\}$ can be regarded as an orthonormal basis with respect to the measure $dF_b(y)$. Therefore, the approximated PDF $\tilde{f}_N(y)$ in (25) is in fact a linear combination of the orthonormal basis and η_l can be regarded as the coordinate of $\tilde{f}_N(y)$ with respect to the basis vector $\mathbf{c}_l^T \mathbf{y}_l$. The expression in (25) will facilitate the analysis of the convergence of $\tilde{f}_N(y)$ with respect to N and enable an efficient selection of the approximation degree N , which will be discussed later.

Based on Theorem 2, the PDF $\tilde{f}_N(y)$ now can be derived. To proceed, the base density function $f_b(y)$ should be determined first. As shown in Theorem 1, the base density function $f_b(y)$ should be chosen to be nontrivial with inverse moments ν_k existing. Notice that the base density function $f_b(y)$ is equivalent to the approximated PDF $\tilde{f}_N(y)$ when the approximation degree is set as zero, i.e., $f_{Y_K^D}(y) \approx \tilde{f}_N(y) = f_b(y)$ when $N = 0$. The base density function $f_b(y)$ should be chosen somewhat close to $f_{Y_K^D}(y)$ [23], [24]. Since the logarithm of Y_K^D can be written as a sum of RVs, i.e., $\ln Y_K^D = \sum_{l=1}^K \ln(1 + \gamma_{SD,l})$, $\ln Y_K^D$ can be roughly approximated as a Gaussian RV based on the central limit theorem when the number of transmissions is large. It is thus natural to choose $f_b(y)$ as the PDF of a Lognormal RV given by

$$f_b(y) = \frac{1}{y\sqrt{2\pi\sigma^2}} e^{-\frac{(\ln y - \mu)^2}{2\sigma^2}}, \quad y \in (0, \infty), \quad (31)$$

where μ and σ^2 represent the mean and the covariance of $\ln(Y_K^D)$, respectively. As shown in Appendix F, the mean μ and the variance σ^2 can be derived as

$$\mu = \sum_{l=1}^K \underbrace{\frac{1}{\Gamma(m)} G_{2,3}^{3,1} \left(\begin{matrix} 0,1 \\ 0,0,m \end{matrix} \middle| \frac{m}{\Omega'_{SD,l}} \right)}_{\triangleq \mu_l}, \quad (32)$$

¹Herein, $(\mathbb{R}, \mathcal{F}, \mu)$ is a measure space, where \mathcal{F} is σ -algebra over \mathbb{R} .

$$\sigma^2 \approx \sum_{l=1}^K \left(\frac{1}{\Gamma(m)} e^{\frac{m}{\Omega'_{SD,l}}} \sum_{p=1}^{N_Q} w_p \ln^2 \left(1 + \frac{\Omega'_{SD,l}}{m} \zeta_p \right) - \mu_l^2 \right) + 2 \sum_{i < j} \left(\frac{\prod_{l=i,j} w_{p_l} \ln \left(1 + \frac{\Omega'_{SD,l} (1 - \lambda_{SD,l}^2)}{m} \zeta_{p_l} \right)}{\Gamma(m) \left(1 + \sum_{l=i,j} \frac{\lambda_{SD,l}^2}{1 - \lambda_{SD,l}^2} \right)^m} \right) \times \Psi_2^{(2)} \left(m; m, m; \varpi_{i,j}^i \zeta_{p_i}, \varpi_{i,j}^j \zeta_{p_j} \right) - \mu_i \mu_j \right), \quad (33)$$

where $G_{p,q}^{m,n}(\cdot)$ represents Meijer G-function [17, 9.301] and $\varpi_{i,j}^l = \left(1 + \sum_{k=i,j} \frac{\lambda_{SD,k}^2}{1 - \lambda_{SD,k}^2} \right)^{-1} \frac{\lambda_{SD,l}^2}{1 - \lambda_{SD,l}^2}$.

Given the base density function $f_b(y)$ in (31), its k th inverse moment ν_k directly follows as

$$\nu_k = \int_0^\infty y^{-k} f_b(y) dy = e^{\frac{k^2 \sigma^2}{2} - k\mu}. \quad (34)$$

The exponential form of ν_k then enables the derivation of the element in the vector \mathbf{c}_l (27) in a closed-form as

$$c_{l,k} = \frac{(-1)^{l+k} e^{k\mu} \zeta^{\frac{k-l-2k^2}{2}} \sqrt{\prod_{l-1 \geq t \geq 0} (1 - \zeta^{t-l})}}{\prod_{t=0, t \neq k}^l (1 - \zeta^{-|t-k|})}, \quad (35)$$

where $\zeta = e^{\sigma^2}$, as proved in Appendix G.

Now putting (16), (26), (31) and (35) into (25), the approximated PDF $\tilde{f}_N(y)$ can be derived. Specifically, it can be written as

$$\begin{aligned} \tilde{f}_N(y) &= f_b(y) \sum_{l=0}^N \eta_l \sum_{k=0}^l c_{l,k} y^{-k} \\ &= \sum_{k=0}^N \sum_{l=k}^N \eta_l c_{l,k} y^{-k-1} \frac{1}{\sqrt{2\pi\sigma^2}} e^{-\frac{(\ln y - \mu)^2}{2\sigma^2}}. \end{aligned} \quad (36)$$

Accordingly, the approximated CDF $\tilde{F}_N(y)$ can be obtained as

$$\begin{aligned} \tilde{F}_N(y) &= \sum_{k=0}^N \sum_{l=k}^N \eta_l c_{l,k} \nu_k \Phi \left(\frac{\ln(y) + k\sigma^2 - \mu}{\sigma} \right) \\ &= \sum_{k=0}^N \kappa_k \Phi \left(\frac{\ln(y) + k\sigma^2 - \mu}{\sigma} \right), \end{aligned} \quad (37)$$

where $\Phi(\cdot)$ denotes the CDF of a standard normal RV and $\kappa_k = \sum_{l=k}^N \eta_l c_{l,k} \nu_k$. Clearly, $\sum_{k=0}^N \kappa_k = 1$ since $F_N(\infty) = 1$. It means that the approximated CDF $\tilde{F}_N(y)$ in fact is a weighted sum of the CDFs of Lognormal RVs.

By plugging (37) into (13), the conditional outage probability $P_{out}(K|BC = K)$ can be derived as

$$\begin{aligned} P_{out}(K|BC = K) &\approx \tilde{F}_N(2^R) \\ &= \sum_{k=0}^N \kappa_k \Phi \left(\frac{C\mathcal{R} + k\sigma^2 - \mu}{\sigma} \right), \end{aligned} \quad (38)$$

where $C = \ln 2$.

This inverse moment matching method can be applied to deriving the distributions of Y_r^R and $Y_{K,r}^D$. Clearly in

the derivation, it is essential to determine their inverse moments, and the mean and variance of their natural logarithms. Since $(\gamma_{SR,1}, \dots, \gamma_{SR,M})$ follows a similar multivariate Gamma distribution with generalized correlation as $(\gamma_{SD,1}, \dots, \gamma_{SD,M})$, the inverse moments of Y_r^R , and the mean and variance of $\ln Y_r^R$ can be derived respectively as (16), (32) and (33) but with the subscript SD replaced as SR . Then the probability $\Pr(BC = r)$ can be obtained by putting the CDF of Y_r^R into (15). With respect to $Y_{K,r}^D$, it can be written as a product of two independent RVs, i.e., $Y_{K,r}^D \triangleq Y_1 Y_2$, where $Y_1 = \prod_{l=1}^r (1 + \gamma_{SD,l})$ and $Y_2 = \prod_{l=r+1}^K (1 + \gamma_{RD,l})$. Due to the independence of Y_1 and Y_2 , the inverse moments of $Y_{K,r}^D$ are given by

$$\mathbb{E}\left(Y_{K,r}^D^{-k}\right) = \mathbb{E}\left(Y_1^{-k}\right) \mathbb{E}\left(Y_2^{-k}\right) = \tilde{\alpha}_{1,k} \tilde{\alpha}_{2,k}, \quad (39)$$

where $\tilde{\alpha}_{1,k}$ and $\tilde{\alpha}_{2,k}$ denote the k th inverse moments of Y_1 and Y_2 , respectively, which can be obtained similarly to (16). Meanwhile, the mean and the variance of $\ln Y_{K,r}^D$ can be obtained as

$$\mathbb{E}\left(\ln Y_{K,r}^D\right) = \mathbb{E}\left(\ln Y_1\right) + \mathbb{E}\left(\ln Y_2\right) = \tilde{\mu}_1 + \tilde{\mu}_2, \quad (40)$$

$$\text{Var}\left(\ln Y_{K,r}^D\right) = \text{Var}\left(\ln Y_1\right) + \text{Var}\left(\ln Y_2\right) = \tilde{\sigma}_1^2 + \tilde{\sigma}_2^2, \quad (41)$$

where $(\tilde{\mu}_1, \tilde{\sigma}_1^2)$ and $(\tilde{\mu}_2, \tilde{\sigma}_2^2)$ denote the mean and the variance of $\ln Y_1$ and $\ln Y_2$, respectively, which can be obtained similarly to (32) and (33). Using the inverse moment matching method, the CDF of $Y_{K,r}^D$ can be finally derived as

$$F_{Y_{K,r}^D}(y) \approx \sum_{k=0}^N \tilde{\kappa}_k \Phi\left(\frac{\ln(y) + k(\tilde{\sigma}_1^2 + \tilde{\sigma}_2^2) - (\tilde{\mu}_1 + \tilde{\mu}_2)}{\sqrt{\tilde{\sigma}_1^2 + \tilde{\sigma}_2^2}}\right), \quad (42)$$

where $\tilde{\kappa}_0, \tilde{\kappa}_1, \dots, \tilde{\kappa}_N$ define the corresponding weightings of Lognormal CDFs. Then the conditional probability $P_{out}(K|BC = r)$ for $r < K$ can be obtained accordingly. Together with the probability of $\Pr(BC = r)$, the outage probability in (9) directly follows.

B. Selection of Approximation Degree

In the inverse moment matching method, an truncation approximation is involved and the approximation degree N should be properly chosen. To this end, the coordinates η_l with respect to the orthonormal basis $\{\mathbf{c}_l^T \mathbf{y}_l, l \in \mathbb{N}\}$ should be analyzed. Recalling $\alpha_n \in (0, 1]$ and putting (35) into (26), we have

$$\begin{aligned} |\eta_N| &\leq \frac{\zeta^{-\frac{N}{2}}}{\phi^2(\zeta^{-1})} \sum_{k=0}^N e^{\sigma^2 k((\mu\sigma^{-2} + \frac{1}{2}) - k)} \\ &\leq (N+1) \zeta^{-\frac{N}{2}} \frac{\zeta^{k_0((\mu\sigma^{-2} + \frac{1}{2}) - k_0)}}{\phi^2(\zeta^{-1})} = A(N+1) \zeta^{-\frac{N}{2}}, \end{aligned} \quad (43)$$

where $k_0 = \frac{\mu\sigma^{-2}}{2} + \frac{1}{4}$, $\phi(q)$ denotes Euler function as $\phi(q) = \prod_{k=1}^{\infty} (1 - q^k)$ and $A = \frac{\zeta^{k_0((\mu\sigma^{-2} + \frac{1}{2}) - k_0)}}{\phi^2(\zeta^{-1})}$. Clearly, η_N approaches to zero as N tends to infinity, which justifies the truncation approximation.

To characterize the error between the PDF $f_{Y_K^D}(y)$ and its approximate $\tilde{f}_N(y)$ in (25), a normalized error is generally defined as [24]

$$\epsilon_N(y) \triangleq \frac{f_{Y_K^D}(y) - \tilde{f}_N(y)}{f_b(y)} = \sum_{l=N+1}^{\infty} \eta_l \mathbf{c}_l^T \mathbf{y}_l. \quad (44)$$

Accordingly, the normalized mean square error (NMSE) is defined as [24]

$$\begin{aligned} \|\epsilon_N(y)\|^2 &\triangleq \langle \epsilon_N(y), \epsilon_N(y) \rangle = \int_0^{\infty} \left(\sum_{l=N+1}^{\infty} \eta_l \mathbf{c}_l^T \mathbf{y}_l \right)^2 dF_b(y) \\ &= \sum_{l=N+1}^{\infty} \sum_{k=N+1}^{\infty} \eta_l \eta_k \langle \mathbf{c}_l^T \mathbf{y}_l, \mathbf{c}_k^T \mathbf{y}_k \rangle = \sum_{l=N+1}^{\infty} \eta_l^2. \end{aligned} \quad (45)$$

Applying the upper bound (43) into (45), it follows that

$$\begin{aligned} \|\epsilon_N(y)\|^2 &\leq \sum_{l=N+1}^{\infty} \left(A(l+1) \zeta^{-\frac{l}{2}} \right)^2 \\ &= A^2 \zeta^{-N} \sum_{l=1}^{\infty} (l+N+1)^2 \zeta^{-l} \\ &= A^2 \zeta^{-N} \left(\frac{\zeta^{-2} + \zeta^{-1}}{(1-\zeta^{-1})^3} + (N+1)^2 \frac{\zeta^{-1}}{1-\zeta^{-1}} \right) \\ &\leq A^2 (N+1)^2 \zeta^{-N} \frac{\zeta^{-1}}{1-\zeta^{-1}} \left(\frac{1+\zeta^{-1}}{(1-\zeta^{-1})^2} + \frac{2}{1-\zeta^{-1}} + 1 \right), \end{aligned} \quad (46)$$

where the last equality holds by using [17, Eq.0.112, Eq.0.113, Eq.0.114]. To guarantee the approximation accuracy, the NMSE should be limited to a small threshold ε , i.e., $\|\epsilon_N(y)\|^2 \leq \varepsilon$. To meet this error constraint and by defining $B = A^2 \frac{\zeta^{-1}}{1-\zeta^{-1}} \left(\frac{1+\zeta^{-1}}{(1-\zeta^{-1})^2} + \frac{2\zeta^{-1}}{(1-\zeta^{-1})} + 1 \right)$, the approximation degree N should be chosen to satisfy

$$B(N+1)^2 \zeta^{-N} \leq \varepsilon. \quad (47)$$

It follows that

$$(N+1) \ln \sqrt{\zeta^{-1}} e^{(N+1) \ln \sqrt{\zeta^{-1}}} \geq \sqrt{\frac{\varepsilon}{B}} \ln \sqrt{\zeta^{-1}} e^{\ln \sqrt{\zeta^{-1}}}. \quad (48)$$

By the definition of Lambert W function, we have

$$(N+1) \ln \sqrt{\zeta^{-1}} \leq W_{-1} \left(\sqrt{\frac{\varepsilon}{B}} \ln \sqrt{\zeta^{-1}} e^{\ln \sqrt{\zeta^{-1}}} \right), \quad (49)$$

where $W_{-1}(\cdot)$ denotes the lower branch of Lambert W function [30, 4.13]. It means that

$$\begin{aligned} N &\geq \frac{W_{-1} \left(\sqrt{\frac{\varepsilon}{B}} \ln \sqrt{\zeta^{-1}} e^{\ln \sqrt{\zeta^{-1}}} \right)}{\ln \sqrt{\zeta^{-1}}} - 1 \\ &= \frac{W_{-1} \left(-\sigma^2/2 \sqrt{\frac{\varepsilon}{B}} e^{-\sigma^2/2} \right)}{-\sigma^2/2} - 1 \triangleq \bar{N}. \end{aligned} \quad (50)$$

For illustration, the approximation degree \bar{N} under various NMSE constraints ε is shown in Fig. 2, by taking a system with parameters $m = 6$, $\Omega_{SD,l}^l = 1$ and $\rho_{SD}^{l,k} = 0.5$ as an

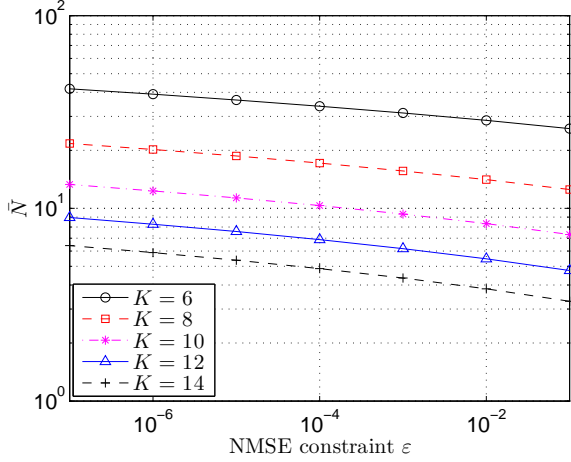


Fig. 2. The approximation degree \bar{N} versus NMSE constraint ε .

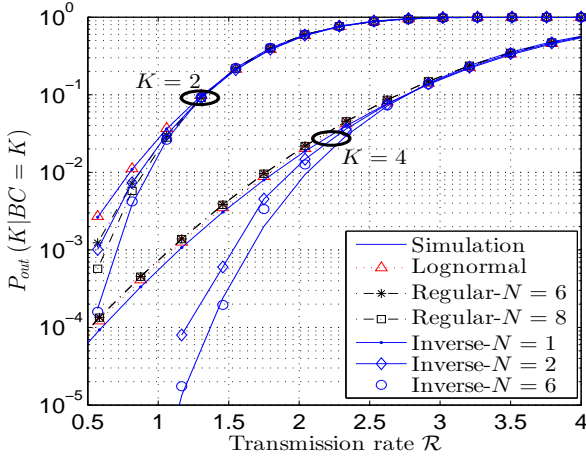


Fig. 3. Effect of approximation degree on $P_{out}(K|BC=K)$.

example. Clearly, the approximation degree \bar{N} decreases when higher NMSE is allowed.

To verify the inverse moment matching method, $P_{out}(K|BC=K)$ and $P_{out}(K|BC=r)$ with $r < K$ are plotted respectively in Fig. 3 and Fig. 4, taking a system with $m = 6$, $\Omega'_{SD,l} = 1$, $\Omega'_{RD,l} = 2$, $r = 2$ and $\rho_{SD}^{l,k} = \rho_{RD}^{l,k} = 0.5$ as an example. Clearly, the gap between the analytical results and Monte Carlo simulation results significantly reduces with N . When $N = 6$, the analytical result coincides well with simulation results, which validates its accuracy. In addition, the proposed inverse moment matching method performs better than the other two approaches, i.e., Lognormal approximation [13] and regular moment matching method [23], [24]². Thus it justifies the effectiveness of the proposed method.

²The regular moment matching method approximates the CDF of Y_K^D as $f_{Y_K^D}(y) \approx f_b(y) \sum_{l=0}^N \tilde{\xi}_{N,l} y^l$ where $f_b(y)$ is chosen as the PDF of a Lognormal RV with mean $-\mu$ and variance σ^2 while the coefficient $\tilde{\xi}_{N,l}$ is determined by matching the first N moments of Y_K^D . Since the moment generation function of Y_K^D do not exist, this method cannot guarantee the uniqueness of the CDF, thus limiting the approximation accuracy.

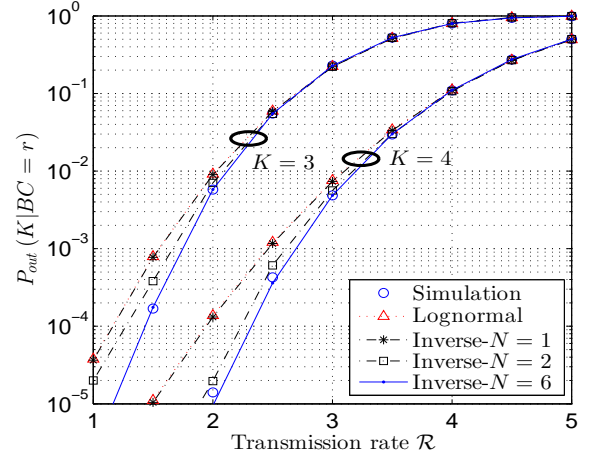


Fig. 4. Effect of approximation degree on $P_{out}(K|BC=r)$ with $r = 2$.

IV. DIVERSITY ORDER

To better understand the behavior of cooperative HARQ-IR schemes, another important performance metric (i.e., diversity order) is also analyzed here. Without loss of generality, the transmission SNR in each HARQ round is set equal, i.e., $P_{S,l}/\mathfrak{N}_{SR,l} = P_{S,l}/\mathfrak{N}_{SD,l} = P_{R,l}/\mathfrak{N}_{RD,l} = \gamma_T$ for $l \in [1, M]$. According to [31], [32], the diversity order d is defined as

$$d = - \lim_{\gamma_T \rightarrow \infty} \frac{\log(P_{out}(M))}{\log(\gamma_T)}. \quad (51)$$

Based on the definition of outage probability in (9) and noticing that the probabilities $\Pr(BC=r)$ are non-negative with $\sum_{r=1}^M \Pr(BC=r) = 1$, we have

$$\begin{aligned} \min \{P_{out}(M|BC=r), r \in [1, M]\} &\leq P_{out}(M) \\ &\leq \max \{P_{out}(M|BC=r), r \in [1, M]\}. \end{aligned} \quad (52)$$

Meanwhile, from the definition of $Y_{K,r}^D \triangleq \prod_{l=1}^r (1 + \gamma_{SD,l}) \times \prod_{l=r+1}^K (1 + \gamma_{RD,l})$ in (13), we also have

$$(1 + \bar{\gamma}_{M,r}) \leq Y_{M,r}^D \leq (1 + M^{-1} \bar{\gamma}_{M,r})^M, \quad (53)$$

where $\bar{\gamma}_{M,r}$ represents the sum of SNRs as $\bar{\gamma}_{M,r} = \sum_{l=1}^r \gamma_{SD,l} + \sum_{l=r+1}^M \gamma_{RD,l}$, and the right inequality follows from the inequality of arithmetic and geometric means. Applying (53) into (13), the conditional outage probability $P_{out}(M|BC=r)$ is found to be bounded as

$$\begin{aligned} F_{\bar{\gamma}_{M,r}} \left(M \left(2^{\frac{R}{M}} - 1 \right) \right) &\leq P_{out}(M|BC=r) \\ &\leq F_{\bar{\gamma}_{M,r}} (2^R - 1), \end{aligned} \quad (54)$$

where $F_{\bar{\gamma}_{M,r}}(\cdot)$ denotes the CDF of $\bar{\gamma}_{M,r}$ and is given by the following theorem.

Theorem 3. The CDF of $\bar{\gamma}_{M,r} = \sum_{l=1}^r \gamma_{SD,l} + \sum_{l=r+1}^M \gamma_{RD,l}$ can be written as

$$\begin{aligned} F_{\bar{\gamma}_{M,r}}(y) &= \frac{y^{Mm}}{\gamma_T^{Mm} (\det(\mathbf{B}))^m \Gamma(Mm+1)} \times \\ &\Phi_2^{(M)} \left(m, \dots, m; Mm+1; -\frac{y}{\gamma_T \delta_1}, \dots, -\frac{y}{\gamma_T \delta_M} \right), \end{aligned} \quad (55)$$

where $\Phi_2^{(M)}(\cdot)$ denotes the confluent Lauricella function [28, Def. A.19], $\{\delta_k\}_{k=1}^M$ are defined as the eigenvalues of the matrix $\mathbf{B} = \mathbf{F}\mathbf{E}$, \mathbf{F} is an $M \times M$ diagonal matrix with diagonal entries as $\{\Omega_{SD,1}/m, \dots, \Omega_{SD,r}/m, \Omega_{RD,r+1}/m, \dots, \Omega_{RD,M}/m\}$, and \mathbf{E} is an $M \times M$ symmetric positive definite matrix given by (56), shown at the top of this page.

Proof. Under time-correlated fading channels, the SNRs in multiple HARQ rounds corresponding to one link are correlated, i.e., $\{\gamma_{SD,1}, \dots, \gamma_{SD,r}\}$ are correlated and $\{\gamma_{RD,r+1}, \dots, \gamma_{RD,M}\}$ are correlated. The moment generating functions (MGFs) of the sum of correlated RVs, i.e., $\sum_{l=1}^r \gamma_{SD,l}$ and $\sum_{l=r+1}^M \gamma_{RD,l}$, can be derived as [33, Eq. 8]. Since $\sum_{l=1}^r \gamma_{SD,l}$ and $\sum_{l=r+1}^M \gamma_{RD,l}$ are independent, the MGF of $\tilde{\gamma}_{M,r}$ can be directly written as the product of MGFs of $\sum_{l=1}^r \gamma_{SD,l}$ and $\sum_{l=r+1}^M \gamma_{RD,l}$. Then by applying inverse Laplace transform into the MGF of $\tilde{\gamma}_{M,r}$, the CDF of $\tilde{\gamma}_{M,r}$ can be derived as (55). \square

From (51), (52) and (54), it follows that

$$\begin{aligned} & - \lim_{\gamma_T \rightarrow \infty} \frac{\max \{ \log (F_{\tilde{\gamma}_{M,r}}(\iota)), r \in [1, M] \}}{\log(\gamma_T)} \leq d \leq \\ & - \lim_{\gamma_T \rightarrow \infty} \frac{\min \{ \log (F_{\tilde{\gamma}_{M,r}}(\psi)), r \in [1, M] \}}{\log(\gamma_T)}. \end{aligned} \quad (57)$$

where $\iota = 2^{\mathcal{R}} - 1$ and $\psi = M(2^{M-1}\mathcal{R} - 1)$.

With (55), the first inequality in (57) can be rewritten as

$$d \geq Mm - \max \left\{ \lim_{\gamma_T \rightarrow \infty} \frac{\log \Phi_2^{(M)}\left(m, \dots, m; Mm+1; -\frac{\iota}{\gamma_T \delta_1}, \dots, -\frac{\iota}{\gamma_T \delta_M}\right)}{\log \gamma_T}, r \in [1, M] \right\}. \quad (58)$$

By using the series representation of the confluent Lauricella function [34], the limit of the confluent Lauricella function is reduced as

$$\lim_{\gamma_T \rightarrow \infty} \Phi_2^{(M)}\left(m, \dots, m; Mm+1; -\frac{\iota}{\gamma_T \delta_1}, \dots, -\frac{\iota}{\gamma_T \delta_M}\right) = 1. \quad (59)$$

Putting (59) into (58) yields $d \geq Mm$. Similarly, the second inequality in (57) can be derived as $d \leq Mm$. The diversity order then directly follows as $d = Mm$. Roughly speaking, a Nakagami- m fading channel can be regarded as a set of m parallel independent Rayleigh fading channels. Hereby, for HARQ operating over Nakagami- m fast fading channels, the maximum achievable diversity order equals to the number of independently faded paths that the transmit signal experiences, i.e., $d_{max} = Mm$ [32]. Therefore, it can be concluded that under time-correlated fading channels with $0 \leq \rho_{SD}^{k,l}, \rho_{RD}^{k,l} < 1$, a full diversity order of Mm can be achieved by this cooperative HARQ-IR scheme. Notice that under quasi-static fading channels, i.e., $\rho_{ab}^{k,l} = 1$, since no time diversity can be gained from HARQ retransmissions in

one link, the diversity order reduces to m when $M = 1$ and $2m$ when $M > 1$ ³.

V. NUMERICAL RESULTS AND DISCUSSIONS

The analytical results derived would facilitate performance evaluation and enable optimal design of cooperative HARQ-IR systems over time-correlated Nakagami- m fading channels. For illustration, we take systems with parameters $2\Omega_{SD,l} = \Omega_{SR,l} = \Omega_{RD,l} = 1$ and a constant correlation model [33], [35], [36], i.e., $\rho_{ab}^{l,k} = \rho$ for $1 \leq l \neq k \leq M$ as examples. Unless otherwise stated, the transmission rate and the transmission SNR are set as $\mathcal{R} = 4$ bps/Hz and $\gamma_T = 10$ dB.

A. Outage Performance Evaluation

As shown in Fig. 5, the outage probability $P_{out}(M)$ is plotted for systems with fading order $m = 6$ and two different time correlations, i.e., $\rho = 0.1, 0.6$. It is easily seen that the analytical results match well with simulation results. The increase of the number of transmissions M significantly decreases the outage probability, which demonstrates the benefit of HARQ-IR protocol. Given the number of transmissions $M > 1$, the curves of outage probability under two different correlations become parallel as the transmission SNR γ_T becomes large. Noticing that the outage probability is plotted as logarithmic scale, it means that $\log P_{out}(M)$ decreases at the same speed with the increase of $\log \gamma_T$ no matter what the correlation is. Here for the case of $M = 1$, the curves under two different correlations merge together since only one transmission is allowed and the relay plays no role in the transmission. Moreover, the curves become steeper with the increase of M . These results are consistent with our analysis in Section IV, that is, the diversity order of cooperative HARQ-IR systems is equal to Mm which is irrelevant to the time correlation.

To further investigate the impact of time correlation on outage performance, Fig. 6 shows the outage probability $P_{out}(M)$ against time correlation ρ for $M = 3$. It is shown that the increase of time correlation would cause an outage performance degradation. For instance, the outage probability increases from 10^{-6} to $2 * 10^{-4}$ as ρ increases from 0 to 1 given $m = 6$. It therefore concludes that channel time correlation has a detrimental impact on outage performance.

Noticing that the fading order m is an important parameter to characterize fading channels, the impact of fading order m on outage performance is studied for $\rho = 0.5$ in Fig. 7. Apparently, the increases of fading order would cause the decrease of outage probability. For example, given four transmissions $M = 4$, the outage performance roughly achieves a 30dB gain when the fading order increases from 1 to 3. Thus we can conclude that the increase of fading order m is beneficial to the outage performance, which has been particularly proved in Section IV, that is, the outage probability is directly proportional to γ_T^{-Mm} , i.e., $P_{out}(M) \propto \gamma_T^{-Mm}$.

³The factor 2 comes due to the exploration of spatial diversity from the source and the relay.

$$\mathbf{E} = \begin{bmatrix} 1 & \sqrt{\rho_{SD}^{1,2}} & \cdots & \sqrt{\rho_{SD}^{1,r}} \\ \sqrt{\rho_{SD}^{2,1}} & 1 & \cdots & \sqrt{\rho_{SD}^{2,r}} \\ \vdots & \vdots & \ddots & \vdots \\ \sqrt{\rho_{SD}^{r,1}} & \sqrt{\rho_{SD}^{r,2}} & \cdots & 1 \\ \mathbf{0}_{(M-r) \times r} & \mathbf{0}_{r \times (M-r)} & & \\ & & 1 & \sqrt{\rho_{RD}^{r+1,r+2}} \cdots \sqrt{\rho_{RD}^{r+1,M}} \\ & & \sqrt{\rho_{RD}^{r+2,r+1}} & 1 \cdots \sqrt{\rho_{RD}^{r+2,M}} \\ & & \vdots & \vdots \ddots \vdots \\ & & \sqrt{\rho_{RD}^{M,r+1}} & \sqrt{\rho_{RD}^{M,r+2}} \cdots 1 \end{bmatrix}, \quad 0 \leq \rho_{SD}^{k,l}, \rho_{RD}^{k,l} < 1. \quad (56)$$

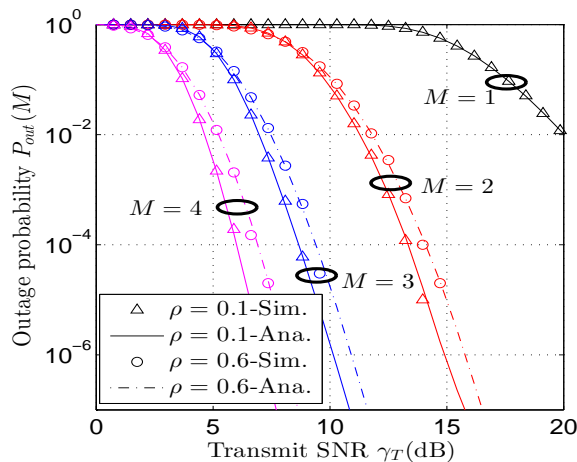


Fig. 5. Verification of analytical results.

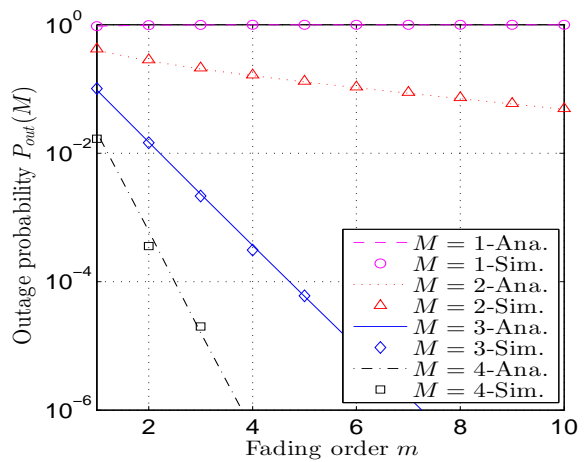


Fig. 7. Impact of fading order.

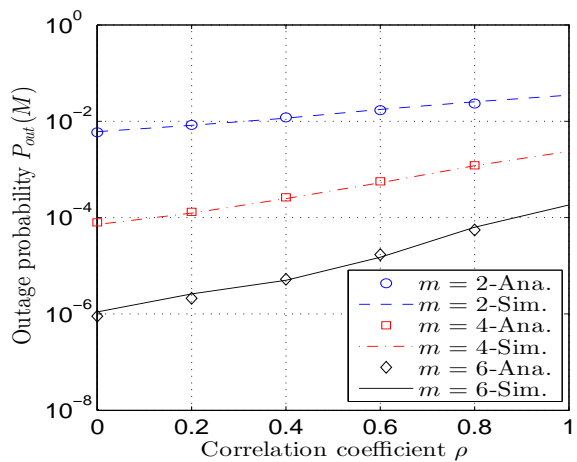


Fig. 6. Impact of time correlation.

B. Optimal Rate Selection

Another widely concerned performance metric for HARQ-IR systems is long term average throughput (LTAT) and it is defined as [18], [37], [38]

$$\bar{\mathcal{T}} = \frac{\mathcal{R}(1 - P_{out}(M))}{1 + \sum_{l=1}^{M-1} P_{out}(l)}. \quad (60)$$

In practice, the HARQ-IR systems should usually be properly designed to achieve the maximum LTAT with guaranteed quality of service, e.g., a specifically low outage probability. Taking the design of the transmission rate as an example, the design problem can be formulated as

$$\max_{\mathcal{R}} \bar{\mathcal{T}} \quad \text{s.t.} \quad P_{out}(M) \leq \vartheta, \quad (61)$$

where ϑ specifies the outage constraint and denotes the maximum allowable outage probability. With our analytical results, the optimal rate and LTAT can be solved easily from (61) by using certain numerical tools. Given the maximum number of transmissions $M = 4$, the optimal LTAT versus the outage constraint ϑ is shown in Fig. 8. It can be seen that the optimal LTAT $\bar{\mathcal{T}}_{opt}$ increases when the outage constraint ϑ is relaxed. However, no significant increase of $\bar{\mathcal{T}}_{opt}$ can be achieved when $\vartheta \geq 10^{-1}$.

VI. CONCLUSIONS

In this paper, we have investigated the performance of cooperative HARQ-IR scheme operating over time-correlated Nakagami- m fading channels. An efficient inverse moment matching method has been proposed to approximate the outage probability in closed-form as a weighted sum of multiple CDFs of Lognormal RVs. In addition, diversity order of cooperative

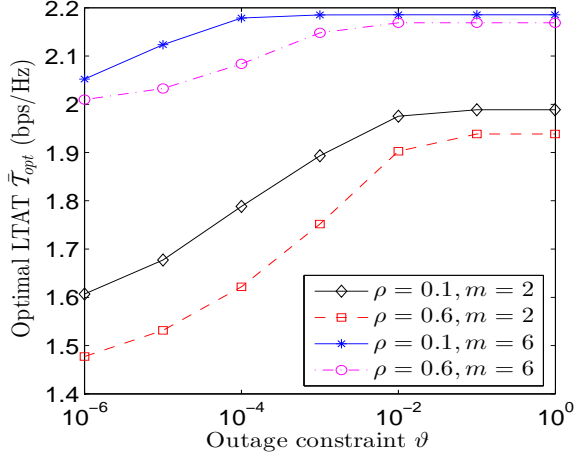


Fig. 8. Optimal LTAT \bar{T}_{opt} against outage constraint ϑ .

HARQ-IR has been analyzed and it has been proved that full diversity can be achieved even under time correlated fading channels except quasi-static fading channels. The numerical results have demonstrated that high fading order and low time correlation are beneficial to the cooperative HARQ-IR scheme.

APPENDIX A

NONEXISTENCE OF MGFs CORRESPONDING TO $Y_{K,r}^D$, Y_K^D ,
AND Y_r^R

The nonexistence of MGFs with respect to $Y_{K,r}^D$, Y_K^D , and Y_r^R can be proved by taking Y_K^D as an example. Since Y_K^D has finite moments of all order, its MGF can be written as [39]

$$\mathcal{M}_{Y_K^D}(s) = \sum_{n=0}^{\infty} \frac{\beta_n s^n}{n!}, \quad (62)$$

where β_n refers to the n th order moment of Y_K^D given as

$$\beta_n = \int_{\gamma_1=0}^{\infty} \cdots \int_{\gamma_K=0}^{\infty} \prod_{l=1}^K (1 + \gamma_l)^n \times f_{\gamma_{SD}^{1:K}}(\gamma_1, \dots, \gamma_K) d\gamma_1 \cdots d\gamma_K. \quad (63)$$

where $\gamma_{SD}^{1:K} = (\gamma_{SD,1}, \dots, \gamma_{SD,K})$ with joint PDF denoted as $f_{\gamma_{SD}^{1:K}}(\gamma_1, \dots, \gamma_K)$. By substituting (8) into (63) and making a change of variable $z_l = m\gamma_{SD,l}/(\Omega'_{SD,l}(1 - \lambda_{SD,l}^2))$, we have

$$\beta_n = \int_{t=0}^{\infty} \frac{t^{m-1}}{\Gamma^{K+1}(m)} e^{-\left(1 + \sum_{l=1}^K \frac{\lambda_{SD,l}^2}{1 - \lambda_{SD,l}^2}\right)t} \times \prod_{l=1}^K \int_0^{\infty} z_l^{m-1} e^{-z_l} \left(1 + \frac{\Omega'_{SD,l}(1 - \lambda_{SD,l}^2)z_l}{m}\right)^n \times {}_0F_1\left(; m; \frac{\lambda_{SD,l}^2 t}{1 - \lambda_{SD,l}^2} z_l\right) dz_l dt. \quad (64)$$

Since ${}_0F_1(; m; t) \geq 1$ for $t \geq 0$, the n th order moment β_n is lower bounded by

$$\beta_n \geq \int_{t=0}^{\infty} \frac{t^{m-1}}{\Gamma^{K+1}(m)} e^{-\left(1 + \sum_{l=1}^K \frac{\lambda_{SD,l}^2}{1 - \lambda_{SD,l}^2}\right)t} dt \times \prod_{l=1}^K \left(\frac{\Omega'_{SD,l}(1 - \lambda_{SD,l}^2)}{m}\right)^n \int_0^{\infty} z_l^{m+n-1} e^{-z_l} dz_l. \quad (65)$$

By using [17, eq. 3.381.4], it follows that

$$\beta_n \geq \left(1 + \sum_{l=1}^K \frac{\lambda_{SD,l}^2}{1 - \lambda_{SD,l}^2}\right)^{-m} \frac{\Gamma^K(m+n)}{\Gamma^K(m)} \times \left(\prod_{l=1}^K \frac{\Omega'_{SD,l}(1 - \lambda_{SD,l}^2)}{m}\right)^n. \quad (66)$$

From (66), the following lower bound of $\beta_n s^n/n!$ holds

$$\frac{\beta_n s^n}{n!} \geq \left(1 + \sum_{l=1}^K \frac{\lambda_{SD,l}^2}{1 - \lambda_{SD,l}^2}\right)^{-m} \frac{\Gamma^K(m+n)}{\Gamma^K(m)n!} \times \left(s \prod_{l=1}^K \frac{\Omega'_{SD,l}(1 - \lambda_{SD,l}^2)}{m}\right)^n \triangleq a_n, \quad (67)$$

Since

$$\lim_{n \rightarrow \infty} \frac{a_n}{a_{n-1}} = \lim_{n \rightarrow \infty} \frac{(m+n-1)^K}{n} s \prod_{l=1}^K \frac{\Omega'_{SD,l}(1 - \lambda_{SD,l}^2)}{m} = \infty, \quad K > 1, \quad (68)$$

it is readily found that $\beta_n s^n/n! \geq a_n \rightarrow \infty$ as $n \rightarrow \infty$ if $K > 1$. Hereby, $\mathcal{M}_{Y_K^D}(s)$ in (62) diverges to infinity for any s . In other words, the MGF $\mathcal{M}_{Y_K^D}(s)$ does not exist. Similarly, we can prove that the MGFs of $Y_{K,r}^D$ and Y_r^R do not exist either.

APPENDIX B

DERIVATION OF α_n

With the definition of $Y_K^D \triangleq \prod_{l=1}^K (1 + \gamma_{SD,l})$, the n -th inverse moment of Y_K^D can be written as

$$\alpha_n = \int_{\gamma_1=0}^{\infty} \cdots \int_{\gamma_K=0}^{\infty} \prod_{l=1}^K (1 + \gamma_l)^{-n} \times f_{\gamma_{SD}^{1:K}}(\gamma_1, \dots, \gamma_K) d\gamma_1 \cdots d\gamma_K. \quad (69)$$

Putting (8) into (69) and making a change of variable $z_l = m\gamma_{SD,l}/(\Omega'_{SD,l}(1 - \lambda_{SD,l}^2))$, it yields

$$\alpha_n = \int_{t=0}^{\infty} \frac{t^{m-1}}{\Gamma^{K+1}(m)} e^{-\left(1 + \sum_{l=1}^K \frac{\lambda_{SD,l}^2}{1 - \lambda_{SD,l}^2}\right)t} \times \prod_{l=1}^K \int_0^{\infty} z_l^{m-1} e^{-z_l} \left(1 + \frac{\Omega'_{SD,l}(1 - \lambda_{SD,l}^2)z_l}{m}\right)^{-n} \times {}_0F_1\left(; m; \frac{\lambda_{SD,l}^2 t}{1 - \lambda_{SD,l}^2} z_l\right) dz_l dt. \quad (70)$$

By adopting Generalized Gaussian Quadrature [27], [40], the n -th inverse moment in (70) can be approximated as

$$\begin{aligned} \alpha_n &\approx \int_{t=0}^{\infty} \frac{t^{m-1}}{\Gamma^{K+1}(m)} e^{-\left(1 + \sum_{k=1}^K \frac{\lambda_{SD,k}^2}{1 - \lambda_{SD,k}^2}\right)t} \\ &\quad \times \prod_{l=1}^K \sum_{p_l=1}^{N_Q} w_{p_l} \left(1 + \frac{\Omega'_{SD,l} (1 - \lambda_{SD,l}^2) \zeta_{p_l}}{m}\right)^{-n} \\ &\quad \times {}_0F_1\left(; m; \frac{\lambda_{SD,l}^2}{1 - \lambda_{SD,l}^2} \zeta_{p_l} t\right) dt \\ &= \sum_{p_1, \dots, p_K \in [1, N_Q]} \frac{\prod_{l=1}^K w_{p_l} \left(1 + \frac{\Omega'_{SD,l} (1 - \lambda_{SD,l}^2) \zeta_{p_l}}{m}\right)^{-n}}{\Gamma^{K+1}(m) \left(1 + \sum_{l=1}^K \frac{\lambda_{SD,l}^2}{1 - \lambda_{SD,l}^2}\right)^m} \\ &\quad \times \int_{t=0}^{\infty} t^{m-1} e^{-t} \prod_{l=1}^K {}_0F_1\left(; m; \varpi_l \zeta_{p_l} t\right) dt, \quad (71) \end{aligned}$$

where N_Q is the quadrature order, the weights w_{p_l} and abscissas ζ_{p_l} for N_Q up to 32 are tabulated in [27], and $\varpi_l = \frac{\lambda_{SD,l}^2}{1 - \lambda_{SD,l}^2} \left(1 + \sum_{k=1}^K \frac{\lambda_{SD,k}^2}{1 - \lambda_{SD,k}^2}\right)^{-1}$. The approximation is valid for non-integer m and can achieve a considerably high accuracy when N_Q is sufficiently large [27], [40]. Since the integral in (71) can be derived as

$$\begin{aligned} &\int_{t=0}^{\infty} t^{m-1} e^{-t} \prod_{l=1}^K {}_0F_1\left(; m; \varpi_l \zeta_{p_l} t\right) dt \\ &= \left(\frac{\Gamma(m)}{2\pi i}\right)^K \int_{c_1} \dots \int_{c_K} \frac{\Gamma\left(m - \sum_{l=1}^K s_l\right) \prod_{l=1}^K \Gamma(s_l)}{\prod_{l=1}^K \Gamma(m - s_l) (-\varpi_l \zeta_{p_l})^{s_l}} ds_1 \dots ds_K \\ &= \Gamma^K(m) \Psi_2^{(K)}(m; m, \dots, m; \varpi_1 \zeta_{p_1}, \dots, \varpi_K \zeta_{p_K}), \quad (72) \end{aligned}$$

where $\Psi_2^{(K)}(; ;)$ denotes the confluent form of Lauricella hypergeometric function [28, Definition A.20] [41], the n -th inverse moment (71) is finally derived as (16).

APPENDIX C PROOF OF THEOREM 1

It is clear from [29] that the n -th inverse moment of Y_K^D is equivalent to the n -th moment of a RV $Z = 1/Y_K^D$, i.e.,

$$\begin{aligned} \alpha_n &= \int_0^{\infty} y^{-n} f_{Y_K^D}(y) dy = \int_0^{\infty} z^n f_{Y_K^D}\left(\frac{1}{z}\right) \frac{1}{z^2} dz \\ &= \int_0^{\infty} z^n f_Z(z) dz, \quad (73) \end{aligned}$$

where $f_Z(z)$ is the PDF of Z and satisfies that $f_Z(z) = f_{Y_K^D}(z^{-1}) z^{-2}$. With Property 1 and the result in [26, pp. 176-177], the distribution of Z can be uniquely determined by its moments α_n . By using moment matching method, the PDF of Z can be uniquely expressed as [23], [24]

$$f_Z(z) = f_a(z) \sum_{l=0}^{\infty} \xi_l z^l. \quad (74)$$

where $f_a(z)$ is a nontrivial base density function with moments $\nu_k = \int_0^{\infty} z^k f_a(z) dz$ existing, and ξ_0, ξ_1, \dots denote the

coefficients of the polynomial of z . Since $Y_K^D = 1/Z$, it follows from (74) that

$$\begin{aligned} f_{Y_K^D}(y) &= y^{-2} f_Z(y^{-1}) = y^{-2} f_a(y^{-1}) \sum_{l=0}^{\infty} \xi_l y^{-l} \\ &= f_b(y) \sum_{l=0}^{\infty} \xi_l y^{-l}, \quad (75) \end{aligned}$$

where $f_b(y) \triangleq y^{-2} f_a(y^{-1})$ and in fact is the inverse distribution with respect to $f_a(z)$. Therefore, $f_b(y)$ is a nontrivial function of y and can be regarded as a base density function with inverse moments existing as $\int_0^{\infty} y^{-k} f_b(y) dy = \int_0^{\infty} z^k f_a(z) dz = \nu_k$. According to Lemma 1, since the PDF $f_{Y_K^D}(y)$ can be uniquely determined by matching all the inverse moments, the coefficients ξ_0, ξ_1, \dots should satisfy

$$\alpha_n = \int_0^{\infty} y^{-n} f_b(y) \sum_{l=0}^{\infty} \xi_l y^{-l} dy = \sum_{l=0}^{\infty} \xi_l \nu_{n+l}, \quad n = 0, 1, \dots \quad (76)$$

APPENDIX D PROOF OF THEOREM 2

In general, ξ_N can be written as

$$\xi_N = \begin{bmatrix} \xi_{N-1} \\ 0 \end{bmatrix} + \mathbf{e}_N, \quad (77)$$

where \mathbf{e}_N characterizes the convergence of the coefficients ξ_l when the approximation degree l is increased from $N-1$ to N . With (24) and (77), \mathbf{e}_N can be obtained as

$$\mathbf{e}_N = \xi_N - \begin{bmatrix} \xi_{N-1} \\ 0 \end{bmatrix} = \mathbf{A}_N^{-1} \left(\alpha_N - \mathbf{A}_N \begin{bmatrix} \xi_{N-1} \\ 0 \end{bmatrix} \right), \quad (78)$$

where the second equality holds due to the invertibility of \mathbf{A}_N . From the definition in (23), \mathbf{A}_N can be rewritten as

$$\mathbf{A}_N = \begin{bmatrix} \mathbf{A}_{N-1} & \mathbf{v}_{N-1} \\ \mathbf{v}_{N-1}^T & \nu_{2N} \end{bmatrix}, \quad (79)$$

where $\mathbf{v}_N = [\nu_{N+1} \ \nu_{N+2} \ \dots \ \nu_{2N+1}]^T$. By putting (79) into (78) and using (22), \mathbf{e}_N can be further derived as

$$\begin{aligned} \mathbf{e}_N &= \mathbf{A}_N^{-1} \left(\alpha_N - \begin{bmatrix} \mathbf{A}_{N-1} \xi_{N-1} \\ \mathbf{v}_{N-1}^T \xi_{N-1} \end{bmatrix} \right) \\ &= \mathbf{A}_N^{-1} \begin{bmatrix} \mathbf{0}_N \\ \alpha_N - \mathbf{v}_{N-1}^T \mathbf{A}_{N-1}^{-1} \alpha_{N-1} \end{bmatrix}, \quad (80) \end{aligned}$$

where $\mathbf{0}_N$ represents a null vector with length N .

By applying the inverse of a partitioned matrix [42, 5.16.b] on (79), it yields

$$\begin{aligned} \mathbf{A}_N^{-1} &= \\ &\begin{bmatrix} (\mathbf{A}_{N-1} - \mathbf{v}_{N-1} \nu_{2N}^{-1} \mathbf{v}_{N-1}^T)^{-1} \\ -(\nu_{2N} - \mathbf{v}_{N-1}^T \mathbf{A}_{N-1}^{-1} \mathbf{v}_{N-1})^{-1} \mathbf{v}_{N-1}^T \mathbf{A}_{N-1}^{-1} \\ -(\mathbf{A}_{N-1} - \mathbf{v}_{N-1} \nu_{2N}^{-1} \mathbf{v}_{N-1}^T)^{-1} \mathbf{v}_{N-1} \nu_{2N}^{-1} \\ (\nu_{2N} - \mathbf{v}_{N-1}^T \mathbf{A}_{N-1}^{-1} \mathbf{v}_{N-1})^{-1} \end{bmatrix}. \quad (81) \end{aligned}$$

Using the matrix inversion lemma [42, 5.17], we have

$$\begin{aligned} & (\mathbf{A}_{N-1} - \mathbf{v}_{N-1}\nu_{2N}^{-1}\mathbf{v}_{N-1}^T)^{-1} = \\ & \mathbf{A}_{N-1}^{-1} + \frac{\mathbf{A}_{N-1}^{-1}\mathbf{v}_{N-1}\mathbf{v}_{N-1}^T\mathbf{A}_{N-1}^{-1}}{\nu_{2N} - \mathbf{v}_{N-1}^T\mathbf{A}_{N-1}^{-1}\mathbf{v}_{N-1}}. \end{aligned} \quad (82)$$

Then putting (82) into (81) and after some manipulations, (81) can be eventually transformed into (28).

Plugging (28) into (80), it produces

$$\begin{aligned} \mathbf{e}_N = & \frac{\alpha_N - \mathbf{v}_{N-1}^T\mathbf{A}_{N-1}^{-1}\alpha_{N-1}}{\sqrt{\nu_{2N} - \mathbf{v}_{N-1}^T\mathbf{A}_{N-1}^{-1}\mathbf{v}_{N-1}}} \times \\ & \underbrace{\begin{bmatrix} -\mathbf{A}_{N-1}^{-1}\mathbf{v}_{N-1} \\ \frac{\sqrt{\nu_{2N} - \mathbf{v}_{N-1}^T\mathbf{A}_{N-1}^{-1}\mathbf{v}_{N-1}}}{1} \\ \sqrt{\nu_{2N} - \mathbf{v}_{N-1}^T\mathbf{A}_{N-1}^{-1}\mathbf{v}_{N-1}} \end{bmatrix}}_{\mathbf{c}_N} \end{aligned} \quad (83)$$

and (83) can be further rewritten as

$$\mathbf{e}_N = \mathbf{c}_N^T \alpha_N \mathbf{c}_N = \eta_N \mathbf{c}_N, \quad (84)$$

where $\eta_N = \mathbf{c}_N^T \alpha_N$, $\mathbf{c}_0 = [1]$ and $\eta_0 = 1$. Substituting (84) into (77), it follows that

$$\begin{aligned} \xi_N = & \begin{bmatrix} \xi_{N-1} \\ 0 \end{bmatrix} + \eta_N \mathbf{c}_N = \begin{bmatrix} \xi_{N-2} \\ \mathbf{0}_2 \end{bmatrix} \\ & + \begin{bmatrix} \eta_{N-1} \mathbf{c}_{N-1} \\ 0 \end{bmatrix} + \eta_N \mathbf{c}_N = \dots = \sum_{l=0}^N \begin{bmatrix} \eta_l \mathbf{c}_l \\ \mathbf{0}_{N-l} \end{bmatrix}. \end{aligned} \quad (85)$$

The proof then completes by substituting (85) into (21).

APPENDIX E PROOF OF REMARK 1

With (84), $\langle \mathbf{c}_l^T \mathbf{y}_l, \mathbf{c}_k^T \mathbf{y}_k \rangle$ can be written as

$$\begin{aligned} & \langle \mathbf{c}_l^T \mathbf{y}_l, \mathbf{c}_k^T \mathbf{y}_k \rangle \\ & = \int_{-\infty}^{\infty} f_b(y) \mathbf{c}_l^T \mathbf{y}_l \mathbf{y}_k^T \mathbf{c}_k dy = \eta_l^{-1} \eta_k^{-1} \mathbf{e}_l^T \mathbf{A}_{l,k} \mathbf{e}_k \\ & = \eta_l^{-1} \eta_k^{-1} \begin{bmatrix} \mathbf{0} & \alpha_l - \mathbf{v}_{l-1}^T \mathbf{A}_{l-1}^{-1} \alpha_{l-1} \\ \alpha_k - \mathbf{v}_{k-1}^T \mathbf{A}_{k-1}^{-1} \alpha_{k-1} \end{bmatrix} \\ & \times \mathbf{A}_l^{-1} \mathbf{A}_{l,k} \mathbf{A}_k^{-1} \begin{bmatrix} \mathbf{0} \\ \alpha_k - \mathbf{v}_{k-1}^T \mathbf{A}_{k-1}^{-1} \alpha_{k-1} \end{bmatrix}, \end{aligned} \quad (86)$$

where

$$\mathbf{A}_{l,k} = \begin{bmatrix} \nu_0 & \nu_1 & \dots & \nu_k \\ \nu_1 & \nu_2 & \dots & \nu_{k+1} \\ \vdots & \vdots & \ddots & \vdots \\ \nu_l & \nu_{l+1} & \dots & \nu_{l+k} \end{bmatrix}, \quad (87)$$

and the last step holds by using (80).

For the case with $l = k$, $\mathbf{A}_{l,k} = \mathbf{A}_l$. It follows from (28) and (86) that

$$\begin{aligned} \langle \mathbf{c}_l^T \mathbf{y}_l, \mathbf{c}_l^T \mathbf{y}_l \rangle & = \eta_l^{-2} \frac{(\alpha_l - \mathbf{v}_{l-1}^T \mathbf{A}_{l-1}^{-1} \alpha_{l-1})^2}{\nu_{2l} - \mathbf{v}_{l-1}^T \mathbf{A}_{l-1}^{-1} \mathbf{v}_{l-1}} \\ & = \eta_l^{-2} |\mathbf{c}_l^T \alpha_l|^2 = 1. \end{aligned} \quad (88)$$

On the other hand, for the case with $l \neq k$, suppose that $l > k$ without loss of generality and then $\mathbf{A}_l^{-1} \mathbf{A}_{l,k} \mathbf{A}_k^{-1}$ can be written as

$$\begin{aligned} \mathbf{A}_l^{-1} \mathbf{A}_{l,k} \mathbf{A}_k^{-1} & = \frac{1}{\det(\mathbf{A}_l) \det(\mathbf{A}_k)} \times \\ & \begin{bmatrix} \mathbf{A}_l^{0,0} & \mathbf{A}_l^{1,0} & \dots & \mathbf{A}_l^{l,0} \\ \mathbf{A}_l^{0,1} & \mathbf{A}_l^{1,1} & \dots & \mathbf{A}_l^{l,1} \\ \vdots & \vdots & \ddots & \vdots \\ \mathbf{A}_l^{0,l} & \mathbf{A}_l^{1,l} & \dots & \mathbf{A}_l^{l,l} \end{bmatrix} \begin{bmatrix} \nu_0 & \nu_1 & \dots & \nu_k \\ \nu_1 & \nu_2 & \dots & \nu_{k+1} \\ \vdots & \vdots & \ddots & \vdots \\ \nu_l & \nu_{l+1} & \dots & \nu_{l+k} \end{bmatrix} \\ & \times \begin{bmatrix} \mathbf{A}_k^{0,0} & \mathbf{A}_k^{1,0} & \dots & \mathbf{A}_k^{k,0} \\ \mathbf{A}_k^{0,1} & \mathbf{A}_k^{1,1} & \dots & \mathbf{A}_k^{k,1} \\ \vdots & \vdots & \ddots & \vdots \\ \mathbf{A}_k^{0,k} & \mathbf{A}_k^{1,k} & \dots & \mathbf{A}_k^{k,k} \end{bmatrix}, \end{aligned} \quad (89)$$

where $\mathbf{A}_l^{i,j}$ denotes the cofactor of the entry in the i -th row and j -th column of \mathbf{A}_l . Applying cofactor expansion of determinants into (89) yields

$$\mathbf{A}_l^{-1} \mathbf{A}_{l,k} \mathbf{A}_k^{-1} = \frac{1}{\det(\mathbf{A}_k)} \begin{bmatrix} \mathbf{A}_k^{0,0} & \mathbf{A}_k^{1,0} & \dots & \mathbf{A}_k^{k,0} \\ \vdots & \vdots & \ddots & \vdots \\ \mathbf{A}_k^{0,k} & \mathbf{A}_k^{1,k} & \dots & \mathbf{A}_k^{k,k} \\ 0 & 0 & 0 & 0 \\ \vdots & \vdots & \vdots & \vdots \\ 0 & 0 & 0 & 0 \end{bmatrix}. \quad (90)$$

Plugging (90) into (86), we have $\langle \mathbf{c}_l^T \mathbf{y}_l, \mathbf{c}_k^T \mathbf{y}_k \rangle = 0$ for $l \neq k$. Then the remark is proved.

APPENDIX F DERIVATION OF μ AND σ^2

A. Mean μ

The mean of RV $\ln(Y_K^D)$ is expressed as

$$\begin{aligned} \mu & = \mathbb{E}(\ln Y_K^D) = \int_0^{\infty} \ln(y) f_{Y_K^D}(y) dy \\ & = \sum_{l=1}^K \int_0^{\infty} \ln(1 + \gamma_l) f_{\gamma_{SD,l}}(\gamma_l) d\gamma_l = \sum_{l=1}^K \mu_l, \end{aligned} \quad (91)$$

where μ_l defines the expectation of $\ln(1 + \gamma_l)$. Since $\gamma_{SD,l} \sim \mathcal{G}(m, \Omega'_{SD,l}/m)$, μ_l is given by

$$\begin{aligned} \mu_l & = \frac{m^m}{(\Omega'_{SD,l})^m \Gamma(m)} \\ & \times \int_0^{\infty} \ln(1 + t) t^{m-1} \exp\left(-\frac{m}{\Omega'_{SD,l}} t\right) dt. \end{aligned} \quad (92)$$

Applying Parseval equality of Meijer G-function [43, Eq. 8.3.21] into (92) produces

$$\begin{aligned} \mu_l & = \frac{m^m}{(\Omega'_{SD,l})^m \Gamma(m)} \int_0^{\infty} t^{m-1} G_{2,2}^{1,2} \left(\begin{matrix} 1,1 \\ 1,0 \end{matrix} \middle| t \right) \\ & \times G_{0,1}^{1,0} \left(\begin{matrix} - \\ 0 \end{matrix} \middle| \frac{m}{\Omega'_{SD,l}} t \right) dt = \frac{1}{\Gamma(m)} G_{2,3}^{3,1} \left(\begin{matrix} 0,1 \\ 0,0,m \end{matrix} \middle| \frac{m}{\Omega'_{SD,l}} \right). \end{aligned} \quad (93)$$

Then by substituting (93) into (91), the mean μ is eventually derived as (32).

B. Variance σ^2

According to the definition of variance of RV $\ln(Y_K^D)$, σ^2 can be expressed as

$$\sigma^2 = \sum_{l=1}^K \text{Var}[\ln(1 + \gamma_{SD,l})] + 2 \sum_{1 \leq i < j \leq K} \text{Cov}(\ln(1 + \gamma_{SD,i}), \ln(1 + \gamma_{SD,j})), \quad (94)$$

where $\text{Var}(\ln(1 + \gamma_{SD,l})) = \text{E}(\ln^2(1 + \gamma_{SD,l})) - \mu_l^2$ and $\text{Cov}(\ln(1 + \gamma_{SD,i}), \ln(1 + \gamma_{SD,j})) = \text{E}(\ln(1 + \gamma_{SD,i}) \ln(1 + \gamma_{SD,j})) - \mu_i \mu_j$.

By making a change of variable $t = m\gamma_{SD,l}/\Omega'_{SD,l}$, $\text{E}(\ln^2(1 + \gamma_{SD,l}))$ is given as

$$\text{E}(\ln^2(1 + \gamma_{SD,l})) = \frac{1}{\Gamma(m)} \exp\left(\frac{m}{\Omega'_{SD,l}}\right) \times \int_0^\infty t^{m-1} e^{-t} \ln^2\left(1 + \frac{\Omega'_{SD,l} t}{m}\right) dt. \quad (95)$$

Using generalized Gaussian quadrature, it can be computed as

$$\text{E}(\ln^2(1 + \gamma_{SD,l})) \approx \frac{1}{\Gamma(m)} e^{\frac{m}{\Omega'_{SD,l}}} \sum_{p=1}^{N_Q} w_p \ln^2\left(1 + \frac{\Omega'_{SD,l} \zeta_p}{m}\right). \quad (96)$$

On the other hand, with (8), $\text{E}(\ln(1 + \gamma_{SD,i}) \ln(1 + \gamma_{SD,j}))$ can be written as

$$\begin{aligned} & \text{E}(\ln(1 + \gamma_{SD,i}) \ln(1 + \gamma_{SD,j})) \\ &= \frac{1}{\Gamma^3(m)} \int_{t=0}^\infty t^{m-1} e^{-\left(1 + \sum_{l=i,j} \frac{\lambda_{SD,l}^2}{1 - \lambda_{SD,l}^2}\right)t} \\ & \times \prod_{l=i,j} \int_0^\infty y_l^{m-1} e^{-y_l} {}_0F_1\left(; m; \frac{\lambda_{SD,l}^2}{1 - \lambda_{SD,l}^2} y_l t\right) \\ & \times \ln\left(1 + \frac{\Omega'_{SD,l} (1 - \lambda_{SD,l}^2)}{m} y_l\right) dy_l dt. \quad (97) \end{aligned}$$

Similar to (71), (97) can be further derived by using the generalized Gaussian quadrature as

$$\begin{aligned} & \text{E}(\ln(1 + \gamma_{SD,i}) \ln(1 + \gamma_{SD,j})) \\ & \approx \sum_{p_i, p_j \in [1, N_Q]} \frac{\prod_{l=i,j} w_{p_l} \ln\left(1 + \frac{\Omega'_{SD,l} (1 - \lambda_{SD,l}^2)}{m} \zeta_{p_l}\right)}{\Gamma^3(m) \left(1 + \sum_{l=i,j} \frac{\lambda_{SD,l}^2}{1 - \lambda_{SD,l}^2}\right)^m} \\ & \times \int_{t=0}^\infty t^{m-1} e^{-t} \prod_{l=i,j} {}_0F_1\left(; m; \varpi_{i,j}^l \zeta_{p_l} t\right) dt, \quad (98) \end{aligned}$$

where $\varpi_{i,j}^l = \left(1 + \sum_{k=i,j} \frac{\lambda_{SD,k}^2}{1 - \lambda_{SD,k}^2}\right)^{-1} \frac{\lambda_{SD,l}^2}{1 - \lambda_{SD,l}^2}$, $l = i, j$.

Then putting (72) into (98) and together with (96), the covariance σ^2 can be obtained as (33).

APPENDIX G DERIVATION OF $c_{l,k}$

Clearly from (27), to derive each element in \mathbf{c}_l , the terms $\nu_{2l} - \mathbf{v}_{l-1}^T \mathbf{A}_{l-1}^{-1} \mathbf{v}_{l-1}$ and $\mathbf{A}_l^{-1} \mathbf{v}_l$ should be determined first.

For the term $\nu_{2l} - \mathbf{v}_{l-1}^T \mathbf{A}_{l-1}^{-1} \mathbf{v}_{l-1}$, by using elementary transformation on the determinant of \mathbf{A}_l^{-1} in (28), we have

$$\det(\mathbf{A}_l^{-1}) = \det\left(\begin{bmatrix} \mathbf{A}_{l-1}^{-1} & \mathbf{0} \\ -\frac{\mathbf{v}_{l-1}^T \mathbf{A}_{l-1}^{-1}}{\nu_{2l} - \mathbf{v}_{l-1}^T \mathbf{A}_{l-1}^{-1} \mathbf{v}_{l-1}} & \frac{1}{\nu_{2l} - \mathbf{v}_{l-1}^T \mathbf{A}_{l-1}^{-1} \mathbf{v}_{l-1}} \end{bmatrix}\right). \quad (99)$$

It then follows that

$$\nu_{2l} - \mathbf{v}_{l-1}^T \mathbf{A}_{l-1}^{-1} \mathbf{v}_{l-1} = \frac{\det(\mathbf{A}_l)}{\det(\mathbf{A}_{l-1})}. \quad (100)$$

With respect to the term $\mathbf{A}_l^{-1} \mathbf{v}_l$, by expressing \mathbf{A}_l^{-1} in terms of cofactors as

$$\mathbf{A}_l^{-1} = \frac{1}{\det(\mathbf{A}_l)} \begin{bmatrix} A_l^{0,0} & A_l^{1,0} & \dots & A_l^{N,0} \\ A_l^{0,1} & A_l^{1,1} & \dots & A_l^{N,1} \\ \vdots & \vdots & \ddots & \vdots \\ A_l^{0,N} & A_l^{1,N} & \dots & A_l^{N,N} \end{bmatrix}, \quad (101)$$

$\mathbf{A}_l^{-1} \mathbf{v}_l$ is rewritten as

$$\mathbf{A}_l^{-1} \mathbf{v}_l = -\frac{1}{\det(\mathbf{A}_l)} \begin{bmatrix} A_{l+1}^{l+1,0} & A_{l+1}^{l+1,1} & \dots & A_{l+1}^{l+1,l} \end{bmatrix}^T, \quad (102)$$

where $A_{l+1}^{i,j}$ denotes the cofactor of the (i, j) -th entry of \mathbf{A}_{l+1} . Thus by plugging (100) and (102) into (27), \mathbf{c}_l is given as

$$\mathbf{c}_l = \frac{1}{\sqrt{\det(\mathbf{A}_l) \det(\mathbf{A}_{l-1})}} \begin{bmatrix} A_l^{l,0} & A_l^{l,1} & \dots & A_l^{l,l} \end{bmatrix}^T. \quad (103)$$

By defining $\mathbf{c}_l = [c_{l,0}, c_{l,1}, \dots, c_{l,l}]$ and using (103), the k th element $c_{l,k}$ can be expressed as

$$c_{l,k} = \frac{A_l^{l,k}}{\sqrt{\det(\mathbf{A}_l) \det(\mathbf{A}_{l-1})}} = \frac{(-1)^{l+k} U_l^{l,k}}{\sqrt{U_l U_{l-1}}}, \quad (104)$$

where $U_l = \det(\mathbf{A}_l)$, and $U_l^{l,k}$ denotes the corresponding minor of $A_l^{l,k}$. With the exponential form of ν_k , both U_l and $U_l^{l,k}$ can be simplified as Vandermonde determinants. Specifically, U_l can be written as

$$\begin{aligned} U_l &= |\nu_{i+j}|_{i,j \in [0,l]} = \left| e^{\frac{(i+j)^2 \sigma^2}{2}} - (i+j)\mu \right|_{i,j \in [0,l]} \\ &= e^{-l(l+1)\mu} \zeta^{\frac{l(l+1)(2l+1)}{6}} |\zeta^{ij}|_{i,j \in [0,l]} \end{aligned} \quad (105)$$

where $\zeta = e^{\sigma^2}$, and the notation $|\nu_{i+j}|_{i,j \in [0,l]}$ represents the determinant of a matrix with ν_{i+j} as its (i, j) -th entry. Clearly, $|\zeta^{ij}|_{i,j \in [0,l]}$ is a Vandermonde determinant, henceforth U_l can be obtained as

$$U_l = e^{-l(l+1)\mu} \zeta^{\frac{l(l+1)(2l+1)}{6}} \prod_{l \geq i > j \geq 0} (\zeta^i - \zeta^j). \quad (106)$$

Similarly, $U_l^{l,k}$ can also be simplified as a Vandermonde determinant given by

$$U_l^{l,k} = e^{\sum_{i=0}^{l-1} \left(\frac{i^2}{2}\sigma^2 - i\mu\right) + \sum_{j=0 \wedge j \neq k}^l \left(\frac{j^2}{2}\sigma^2 - j\mu\right)} \times \left| \varsigma^{ij} \right|_{i \in [0, l-1], j \in [0, l] \wedge j \neq k} \\ = \frac{U_l}{(-1)^{l-k} \nu_l \nu_k \prod_{t=0 \wedge t \neq k}^l (\varsigma^k - \varsigma^t)}. \quad (107)$$

By substituting (106) and (107) into (104), it yields

$$c_{l,k} = \sqrt{\frac{U_l}{U_{l-1}}} \frac{1}{\nu_l \nu_k \prod_{t=0 \wedge t \neq k}^l (\varsigma^k - \varsigma^t)} = \frac{\sqrt{\prod_{l-1 \geq t \geq 0} (\varsigma^l - \varsigma^t)}}{\nu_k \prod_{t=0 \wedge t \neq k}^l (\varsigma^k - \varsigma^t)}. \quad (108)$$

After some algebraic manipulations, (108) is finally simplified as (35).

REFERENCES

- [1] M. Ergen, *Mobile broadband: including WiMAX and LTE*. Springer Science & Business Media, 2009.
- [2] E. Dahlman, S. Parkvall, and J. Skold, *4G: LTE/LTE-advanced for mobile broadband*. Academic press, 2013.
- [3] H. Chen, R. G. Maunder, and L. Hanzo, "A survey and tutorial on low-complexity Turbo coding techniques and a holistic hybrid ARQ design example," *IEEE Commun. Surveys Tuts.*, vol. 15, no. 4, pp. 1546–1566, Feb. 2013.
- [4] B. Maham, A. Behnad, and M. Debbah, "Analysis of outage probability and throughput for half-duplex hybrid-ARQ relay channels," *IEEE Trans. Veh. Technol.*, vol. 61, no. 7, pp. 3061–3070, Sept. 2012.
- [5] I. Stanojev, O. Simeone, Y. Bar-Ness, and D. H. Kim, "Energy efficiency of non-collaborative and collaborative hybrid-ARQ protocols," *IEEE Trans. Wireless Commun.*, vol. 8, no. 1, pp. 326–335, Jan. 2009.
- [6] J. Choi, W. Xing, D. To, Y. Wu, and S. Xu, "On the energy efficiency of a relaying protocol with HARQ-IR and distributed cooperative beamforming," *IEEE Trans. Wireless Commun.*, vol. 12, no. 2, pp. 769–781, Feb. 2013.
- [7] D. Zennaro, S. Tomasin, and L. Vangelista, "Base station selection in uplink macro diversity cellular systems with hybrid ARQ," *IEEE J. Sel. Areas Commun.*, vol. 29, no. 6, pp. 1249–1259, Jun. 2011.
- [8] A. Chelli and M. Alouini, "On the performance of hybrid-ARQ with incremental redundancy and with code combining over relay channels," *IEEE Trans. Wireless Commun.*, vol. 12, no. 8, pp. 3860–3871, Aug. 2013.
- [9] S. M. Kim, W. Choi, T. W. Ban, and D. K. Sung, "Optimal rate adaptation for hybrid ARQ in time-correlated Rayleigh fading channels," *IEEE Trans. Wireless Commun.*, vol. 10, no. 3, pp. 968–979, Mar. 2011.
- [10] H. Jin, C. Cho, N.-O. Song, and D. K. Sung, "Optimal rate selection for persistent scheduling with HARQ in time-correlated Nakagami-m fading channels," *IEEE Trans. Wireless Commun.*, vol. 10, no. 2, pp. 637–647, Feb. 2011.
- [11] T. V. Chaitanya and E. G. Larsson, "Adaptive power allocation for HARQ with chase combining in correlated Rayleigh fading channels," *IEEE Wireless Commun. Lett.*, vol. 3, no. 2, pp. 169–172, Apr. 2014.
- [12] Z. Shi, H. Ding, S. Ma, and K.-W. Tam, "Analysis of HARQ-IR over time-correlated Rayleigh fading channels," *IEEE Trans. Wireless Commun.*, vol. 14, no. 12, pp. 7096–7109, Dec. 2015.
- [13] X. Yang, Z. Shi, S. Ma, and K.-W. Tam, "Performance analysis of cooperative HARQ-IR over time-correlated Nakagami-m fading channels," in *Proc. IEEE International Conference on Communication Systems (ICCS'14)*, Nov. 2014, pp. 404–408.
- [14] L. Szczecinski, S. R. Khosravirad, P. Duhamel, and M. Rahman, "Rate allocation and adaptation for incremental redundancy truncated HARQ," *IEEE Trans. Commun.*, vol. 61, no. 6, pp. 2580–2590, Jun. 2013.
- [15] S. Khosravirad, L. Szczecinski, and F. Labeau, "Rate adaptation for cooperative HARQ," *IEEE Trans. Commun.*, vol. 62, no. 5, pp. 1469–1479, May 2014.
- [16] N. C. Beaulieu and K. T. Hemachandra, "Novel simple representations for Gaussian class multivariate distributions with generalized correlation," *IEEE Trans. Inf. Theory*, vol. 57, no. 12, pp. 8072–8083, Dec. 2011.
- [17] I. S. Gradshteyn, I. M. Ryzhik, A. Jeffrey, D. Zwillinger, and S. Technica, *Table of integrals, series, and products*, 7th ed. Academic press, 2007.
- [18] G. Caire and D. Tuninetti, "The throughput of hybrid-ARQ protocols for the Gaussian collision channel," *IEEE Trans. Inf. Theory*, vol. 47, no. 5, pp. 1971–1988, Jul. 2001.
- [19] P. Wu and N. Jindal, "Performance of hybrid-ARQ in block-fading channels: a fixed outage probability analysis," *IEEE Trans. Commun.*, vol. 58, no. 4, pp. 1129–1141, Apr. 2010.
- [20] T. Tabet, S. Dusad, and R. Knopp, "Diversity-multiplexing-delay trade-off in half-duplex ARQ relay channels," *IEEE Trans. Inf. Theory*, vol. 53, no. 10, pp. 3797–3805, Oct. 2007.
- [21] S. Sesia, G. Caire, and G. Vivier, "Incremental redundancy hybrid ARQ schemes based on low-density parity-check codes," *IEEE Trans. Commun.*, vol. 52, no. 8, pp. 1311–1321, Aug. 2004.
- [22] D. Tse, *Fundamentals of wireless communication*. Cambridge university press, 2005.
- [23] S. B. Provost, "Moment-based density approximants," *Mathematica Journal*, vol. 9, no. 4, pp. 727–756, 2005.
- [24] S. B. Provost and M. Jiang, "Orthogonal polynomial density estimates: alternative representation and degree selection," *International Journal of Computational and Mathematical Sciences*, vol. 5, no. 7, pp. 1089–1096, 2011.
- [25] A. D. Poularikas, *Transforms and applications handbook*. CRC press, 2010.
- [26] H. Cramér, *Mathematical methods of statistics*. Princeton university press, 1999, vol. 9.
- [27] P. Rabinowitz and G. Weiss, "Tables of abscissas and weights for numerical evaluation of integrals of the form $\int_0^\infty e^{-x} x^n f(x) dx$," *Mathematical Tables and Other Aids to Computation*, vol. 13, no. 68, pp. 285–294, Oct. 1959.
- [28] A. Mathai, R. K. Saxena, and H. J. Haubold, *The H-function*. Springer, 2009.
- [29] Z. Govindarajulu, "Theory of inverse moments," DTIC Document, Tech. Rep., 1962.
- [30] F. W. Olver, *NIST handbook of mathematical functions*. Cambridge University Press, 2010.
- [31] A. Chelli, E. Zedini, M.-S. Alouini, J. Barry, and M. Patzold, "Performance and delay analysis of hybrid ARQ with incremental redundancy over double Rayleigh fading channels," *IEEE Trans. Wireless Commun.*, vol. 13, no. 11, pp. 6245–6258, Nov. 2014.
- [32] L. Zheng and D. N. C. Tse, "Diversity and multiplexing: a fundamental tradeoff in multiple-antenna channels," *IEEE Trans. Inf. Theory*, vol. 49, no. 5, pp. 1073–1096, May 2003.
- [33] M.-S. Alouini, A. Abdi, and M. Kaveh, "Sum of Gamma variates and performance of wireless communication systems over Nakagami-fading channels," *IEEE Trans. Veh. Technol.*, vol. 50, no. 6, pp. 1471–1480, Nov. 2001.
- [34] V. Aalo, T. Piboongunon, and G. Eftymoglou, "Another look at the performance of MRC schemes in Nakagami-m fading channels with arbitrary parameters," *IEEE Trans. Commun.*, vol. 53, no. 12, pp. 2002–2005, Dec. 2005.
- [35] V. Aalo *et al.*, "Performance of maximal-ratio diversity systems in a correlated Nakagami-fading environment," *IEEE Trans. Commun.*, vol. 43, no. 8, pp. 2360–2369, Aug. 1995.
- [36] Y. Chen and C. Tellambura, "Distribution functions of selection combiner output in equally correlated Rayleigh, Rician, and Nakagami-m fading channels," *IEEE Trans. Commun.*, vol. 52, no. 11, pp. 1948–1956, Nov. 2004.
- [37] M. Zorzi and R. R. Rao, "On the use of renewal theory in the analysis of ARQ protocols," *IEEE Trans. Commun.*, vol. 44, no. 9, pp. 1077–1081, Sept. 1996.
- [38] B. Zhao and M. C. Valenti, "Practical relay networks: a generalization of hybrid-ARQ," *IEEE J. Sel. Areas Commun.*, vol. 23, no. 1, pp. 7–18, Jan. 2005.
- [39] P. Billingsley, *Probability and measure*. John Wiley & Sons, 2008.
- [40] G. Dahlquist and Å. Björck, *Numerical Methods in Scientific Computing, Volume I*. Society for Industrial and Applied Mathematics, 2008. [Online]. Available: <http://epubs.siam.org/doi/abs/10.1137/1.9780898717785>
- [41] M. Saigo and V. K. Tuan, "Some integral representations of multivariable hypergeometric functions," *Rendiconti del Circolo Matematico di Palermo*, vol. 41, no. 1, pp. 69–80, Jan. 1992.
- [42] K. M. Abadir and J. R. Magnus, *Matrix algebra*. Cambridge University Press, 2005, vol. 1.
- [43] L. Debnath and D. Bhatta, *Integral transforms and their applications*. CRC press, 2010.